Design and Characterizing of Optical Carrier Recovery Scheme

Sachinthani Eranga Alahakoon

(178046A)

Thesis submitted in partial fulfillment of the requirements for the degree
Master of Philosophy

Department of Electronic and Telecommunication Engineering

University of Moratuwa
Sri Lanka

June 2021

Declaration

I declare that this is my work, and this thesis does not incorporate without acknowledgement any material previously submitted for a degree or diploma in any other university or institute of higher learning, and to the best of my knowledge and belief it does not contain any material previously published or written by another person except where the acknowledgement is made in the text.

Also, I hereby grant to University of Moratuwa the non-exclusive right to reproduce and distribute my thesis, in whole or in part, in print, electronic, or any other medium. I retain the right to use this content in whole or part in future works (such as articles or books).

Signature: Date:

The candidate, whose signature appears above, carried out research for the MPhil dissertation under my supervision.

Signature: Date:

Abstract

The field of optical communication has gained rapid development throughout the past years. With the exponentially increasing demand for the internet, the existing transmission bandwidth of fiber optic communication has become insufficient to meet up with end-user requirements. Hence, it is necessary to increase the data rate while enhancing the quality of optical communication systems. Due to the unavailability of high-speed electronics, typical intensity modulation is hard to improve further. One future proof option is to use phase modulated schemes or a combination of phase and amplitude modulation schemes. In this scenario, simultaneous amplitude and phase regeneration schemes are implemented thus making phase synchronization a major concern during the regeneration process. This research is intended to extract the carrier signal phase using the principle of four wave mixing (FWM) and to implement a successful optical carrier recovery scheme. The noise influences from the signal laser for the recovered carrier have been investigated both theoretically and experimentally. Also, the dispersion effects have been analyzed experimentally.

Index terms— Optical fiber communication, carrier recovery, Four Wave Mixing, linewidth, Signal to Noise ratio, binary phase shift keying.

Acknowledgements

I wish to express my deepest and sincere gratitude to my supervisor Prof. L. W. P. R. Udayanga, Professor, Department of Electronic and Telecommunication Engineering, University of Moratuwa for giving me the opportunity to conduct a MPhil under his supervision. I would like to thank him for his guidance throughout the project, his encouragement in difficult situations and his patience with my mistakes.

I like to thank Dr. Tharaka Samarasinghe, Senior Lecturer, Department of Electronic and Telecommunication Engineering, University of Moratuwa and Dr. Vijitha R. Herath, Senior Lecturer, Department of Electrical and Electronic Engineering, University of Peradeniya for their support and ideas during the progress reviews. Also I am thankful to all research assistants and as well as my colleagues in the fiber optic research group for their continuous support. Also, I would like to thank all other friends who helped me directly and indirectly.

Finally, I wish to express my deepest gratitude to my loving parents and my brother for their love and encouragement. I am very much thankful to my husband and his family for their love, understanding and continuous support to complete this research work. To them, I dedicate this report.

This work was financially supported by the National Research Council of Sri Lanka (NRC) (Grant No: 15-146) and Senate Research Committee (SRC) of University of Moratuwa.

Contents

List of Figures

List of Tables

List of Abbreviations

Abbreviation	Description
ASK	Amplitude shift keying
PSK	Phase shift keying
FWM	Four wave mixing
HNLF	Highly non-linear fiber
OSNR	Optical signal to noise ratio
BPSK	Binary phase shift keying
WDM	Wavelength division multiplexing
EDFA	Erbium doped fiber amplifier
LED	Light-emitting diode
LASER	Light amplification by stimulated emission of radiation
FSK	Frequency shift keying
MZM	Mach Zehender modulator
BFSK	Binary frequency shift keying
MFSK	Multilevel frequency shift keying
DPSK	Differential phase shift keying
QPSK	quadrature phase shift keying
FWHM	Full width at half maximum
OSA	Optical signal analyzer
ESA	Electrical signal analyzer
SPM	Self phase modulation
CPM	Cross phase modulation
SRS	Stimulated raman scattering
SBS	Stimulated brillouin scattering
PLL	Phase lock loop
VCO	Voltage controlled oscillator
IL	Injection locking
OSNR	Optical signal to noise ratio
BER	Bit error rate
ISI	Inter symbol interference

ADC	Analog-to-digital converters
OEO	Optical electrical optical
PSA	Phase sensitive amplifier
NMZI	Nonlinear Mach-Zehnder interferometer
NOLM	Nonlinear optical loop mirror
QAM	Quadrature amplitude modulation
SOA	Semiconductor optical amplifiers
SNR	Signal to noise ratio
ASE	Amplified spontaneous emission
AM	Amplitude modulation
PM	Phase modulation
PBRS	Pseudo random bit sequence
ZDW	Zero dispersion wavelength
SMF	Signal mode fiber
LO	Local Oscillator

Chapter 1

INTRODUCTION

Over the years, optical fiber networks have been developed in such a way that the leading internet service providers are replacing their underlying copper cable networks with optical fiber. The optical fiber communication has successfully addressed many issues of conventional communications, however it requires high installation and maintenance costs and requirement of a highly skilled workforce. But the recent surveys show that existing bandwidth is not sufficient to overcome the end-user requirements [7]. The transport networks are upgrading their capacity continuously to provide the bandwidth requirement. As a result, the network capacities have moved from 40 Gbps to 400 Gbps data rate per single channel [8]. While increasing the data rate, the quality of the optical communication system should be preserved. One of the proven methods is to change the modulation scheme from amplitude shift keying (ASK) to phase shift keying (PSK) [9]. The signal processing in the ASK scheme will be no longer effective because, the currently developed optical communication systems are operating based on the PSK scheme.

In any long distance communication system the receiving and recovering the information sent over the channel is required. To recover modulated information at the receiver, as the same quality of the original signal, initiat the carrier information should be recovered. This information which was used for modulation of the optical carrier signal has to be stripped off from the received signal.

Even though phase modulation is a better option for achieving high data rates, signal regeneration in an optical domain has become a challenge. Phase synchronization is a major requirement to achieve accurate and efficient signal reception and regeneration. Hence, it is necessary to extract the original carrier phase information from the incoming phase modulated signal for homodyne receiving process or signal regeneration and synchronization. However, in most of the PSK modulation schemes, a strong carrier is not available. Therefore, various optical carrier recovery methods have been experimented [10–12]. The optical carrier recovery method using four wave mixing (FWM) in a highly non-linear fiber (HNLF) was experimentally demonstrated [13]. However, most of the demonstrated schemes have not done detailed characterization. In this research, it is expected to characterize the extracted recovered carrier with respect to the signal-to-noise ratio degradation and tolerance for accumulated dispersion of the incoming signal. This will help in the process of homodyne receiving, signal regeneration, synchronization, format conversion, etc. The technique used to recover the original carrier during the analysis is FWM. Most communication systems generally try to avoid nonlinear effects but it is useful in this scenario.

Aims and Objectives

Aims and the objectives of this research is divided into 3 sections according to the problem statement.

- Perform Optical Carrier Recovery
- Impact of noise on recovered carrier's linewidth
- Impact of Accumulated dispersion effects on recovered carrier linewidth

1.1 Outline of the Thesis

The organization of the chapters is as follows:

- Chapter 2: Literature Review
  This section summarizes the related research work conducted and different techniques used in optical carrier recovery. Further, it presents the theory including basic concepts in optical communications systems, FWM, BPSK, effects of channel impairments, non-linear phenomena, fiber types and how they are used to effectively transmit data.

- Chapter 3: Optical Carrier Recovery Scheme
  This chapter briefly describes the methodology used to develop a carrier recovery scheme and present the results obtained and analyzes the performance.

- Chapter 4: System Characterization for Degrading OSNR
  This chapter theoretically and experimentally examine the effect of input OSNR of the BPSK modulated signal on the recovered carrier LW. This also includes a comparison of theoretical and experimental results.

- Chapter 5: Characterization for Accumulated Dispersion
  This section presents the effect of the accumulated dispersion value on the recovered carrier, the problems faced and how those were overcome.

- Chapter 6: Conclusion and Future Work
  This chapter details the major findings of this research and the conclusions that can be formed from the results. A subsequent part lists recommendations for further developments is also discussed.

Chapter 2

LITERATURE REVIEW

2.1 Historical Background

Modern optical communication had started with the invention of the ruby laser in 1960 [14]. After a few years of this invention, the low loss optical fibers were invented which was not only used in communication but also gave an encouragement to conduct fundamental research about their properties. Optical communication is the most important application of optical fibers, therefore, most of the research work has been conducted on fiber communication. The low loss fiber (20 dB/km at 632.8 nm) was demonstrated in 1970 [15].

In the first generation of the light-wave system, bit rate was limited to below 100 Mb/s due to the dispersion and multi-mode fiber. The single mode fibers were used as a solution to this limitation [16]. In 1981, they demonstrated a single mode fiber with 2 Gb/s bit rate over 44 km [17]. In the second generation, after 1987, the light-wave system introduced a commercial system with 1.7 Gb/s bit rate with a repeater spacing over 50 km.

Researchers developed fiber technology with loss reduction up to 0.154 dB/km in the past century [18]. Low fiber attenuation is 0.003 dB/km recorded in 2002 [19]. Today, most of the commercially available fiber has 0.2 dB/km attenuation at around 1.55 μm. It is the low loss window of the optical fiber [20]. Because of this low loss characteristic of optical fiber, optical signals can be transmitted for long distances without regeneration and amplification. But in the third generation, they realized that the light-wave systems which operate at 1.55 μm were considerably delayed by large fiber dispersion. This dispersion phenomenon can be overcome by limiting the spectrum to the single longitudinal mode or using dispersion shifted fiber with less dispersion at the 1.55 μm [21]. In 1990, (Third generation light-wave system) the system operating at a bit rate of up to 10 Gb/s were invented commercially. But in the third generation system, electronics repeaters have to be placed at every 60 km to regenerate signals periodically. The repeater space can be increased by improving receiver sensitivity using homodyne or heterodyne detection schemes [21,22]. Such a system is called a coherent light wave system; it is not commercially invented because of the advent of fiber amplifiers in 1989.

The optical amplifier and the wavelength division multiplexing (WDM) were used in the fourth generation system. This optical amplification was used for increasing the repeater spacing and WDM increasing the total capacity in a single fiber. After inventing the WDM technique, the system capacity dramatically increased and led to operating at a bit rate in Tb. The WDM system uses erbium-doped fiber amplifiers (EDFA) spaced 80 km apart to compensate for fiber losses. It helps to transmit data over 21000 km and to develop an amplifier based, all optical, submarine transmission systems for intercontinental communication [23]. Therefore, at the end of the fourth generation system, a huge technological jump of fiber optic communication was achieved. At end of the 2000, there was a commercial terrestrial system with a capacity of 1.6 Tb/s and after a few years, they extended the capacity to nearly 5 Tb/s [24–26].

In the next generation systems wavelength range extended from the conventional wavelength window (C band) to both long and short wavelength windows (L and S band) in which a WDM system that is capable of operating at the same time and increase the bit rate of each window thus rises up the total capacity inside a single fiber. Now, the fiber loss occurs mostly due to the Rayleigh scattering in optical fiber. Optical communication technology has developed due to the rapid development of fibers and optical sources [16,27].

2.2 Theory

2.2.1 Optical fiber communication system

The general communication system includes three basic components, a transmitter or modulator connected to the information source, the transmission medium, and a receiver or demodulator at the destination point. Figure 2.1 shows the schematic diagram of a general communication system. As shown in the figure an electrical signal fed into the transmitter by information source and at the transmitter, that signal gets modulated or converted to any suitable modulation form to transmit over the transmission media (a pair of wires, a coaxial cable or a radio link) by comprising electrical and electronic components in the transmitter. Before the destination, there is a receiver that is used to transform or demodulate the received signal into an original electrical information signal [8, 28, 29].

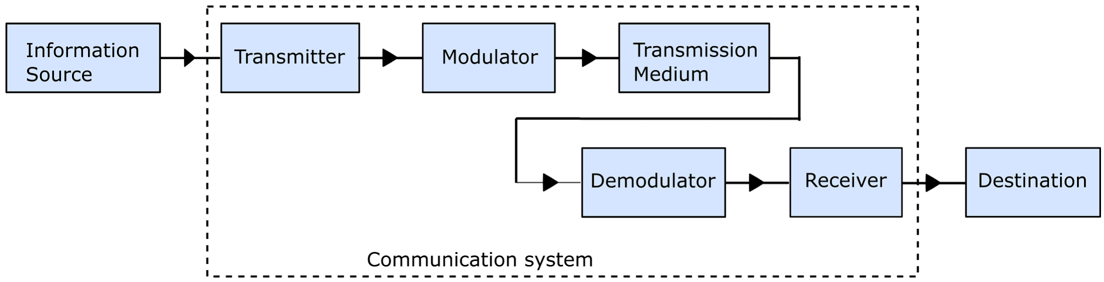

Figure 2.1: Basic Communication System

An optical communication system is similar to a general communication system. In optical communication systems, the three basic components are, an optical transmitter (e.g. an LED or a LASER) to convert electrical signals to optical signals, an optical channel (e.g. fiber optic cable or free space for wireless-optics) and an optical receiver consists with an optical detector (e.g. a photodiode) that operate in electrical domain and demodulate the optical carrier. Since all types of communication signals are generally modulated using a suitable carrier, an optical system also has a modulator (e.g. a Mach-Zehnder or an Electro-absorption Modulator) to modulate the information signal. To aid long distance communication, repeaters or amplifiers are also present (e.g. Erbium Doped Fiber Amplifier). The receiver circuitry, therefore, comprises a demodulator. Sometimes many signals are multiplexed in modern systems (e.g. Wavelength Division Multiplexed Systems) [8,30–32]. Therefore, a multiplexer and a demultiplexer are also needed. A simple optical communication system is depicted in Figure 2.2.

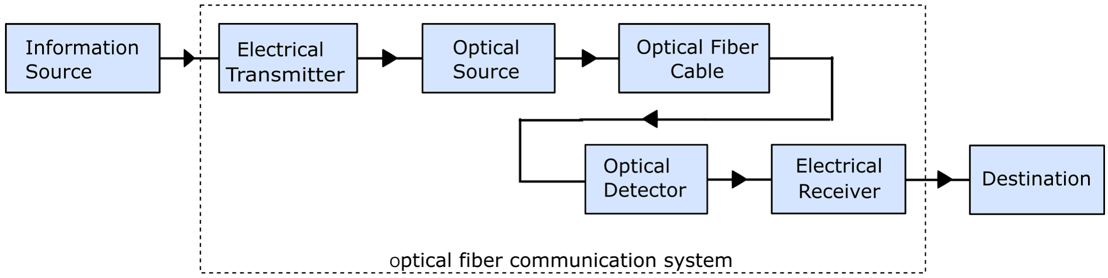

Figure 2.2: Basic Optical Communication System

2.2.2 Optical communication media

The purpose of communication media is to transmit a signal from the transmitter to the receiver. Optical fiber is the most popular communication media in most of the light-wave systems. Silica fiber has the ability to transmit light with small losses as 0.2 dB/km, and only 1% optical power reduction after 100km. Fiber consists of some design issues and those issues determine the repeater or amplifier spacing of long haul lightwave systems. Dispersion is a major issue in optical communication and that causes the broadening of individual optical pulses with propagation. These kinds of issues will lead to inaccurate recovery of the received signal.This problem occurs in the multi mode fibers. Different speeds related to various fiber modes causes the recovery of the received signal to be inaccurate. To overcome this, most optical communication systems use single mode fibers. As shown in figure 2.3 ordinary fibers that are made of glass (SiO2) are exposed to high dispersion and attenuation. Therefore, special kinds of fibers such as dispersion compensated fibers and dispersion shifted fibers are used for compensating the dispersion [8, 16, 33].

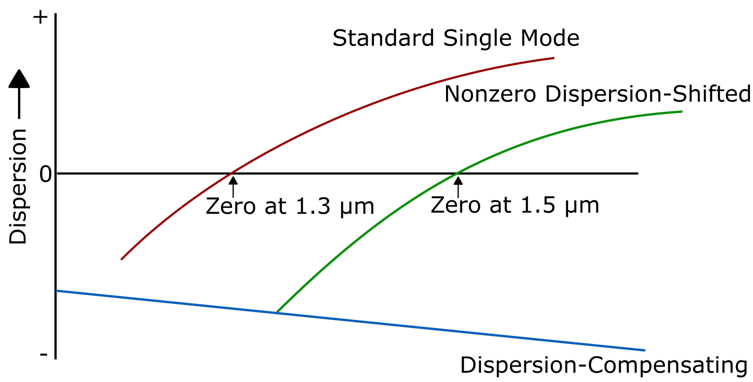

Figure 2.3: Total dispersion in several fiber types [1]

Since these newer fibers have lower loss and attenuation, research about specific fiber types was increased. There are special types of fibers to address some newer issues such as low water peak fiber and large effective (core) area fiber (LEAF). Water peak is a loss feature that is there in SiO2 fibers due to the hydroxyl ions in the fiber cable (Figure 2.4). Therefore, the profile of fiber is shown as a sudden peak which is undesirable in fiber communication systems. By eliminating this effect, the low water peak fiber was invented [2].

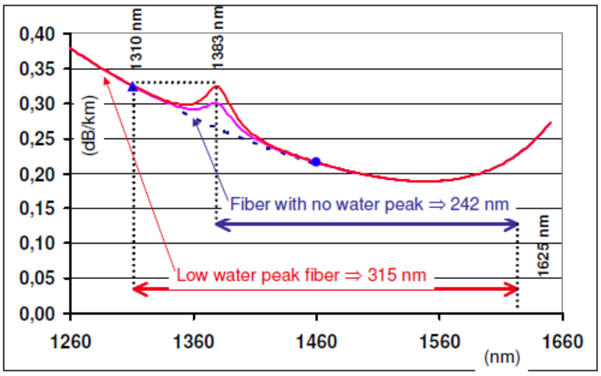

Figure 2.4: Comparison of loss profiles [2]

Fiber which has a large effective (core) area is a fiber type that allows more beam quality and lesser impact from nonlinear effects. These support more modes; therefore these are also called large mode area fibers(Figure 2.5) [16].

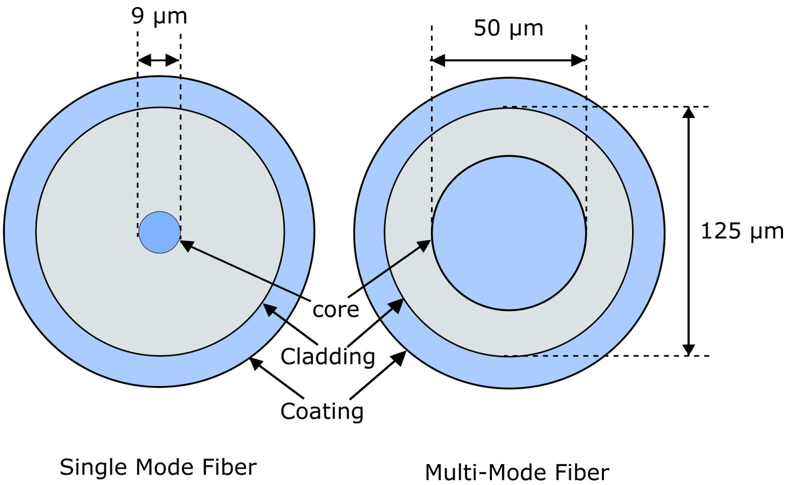

Figure 2.5: Cross section of single and multi-mode fiber

All fibers have a set of special effects called nonlinear effects that are caused due to the refractive indices of the fiber core and cladding plus material used for fiber construction. Generally, these effects reduce the efficiency and signal quality, therefore some compensation is used to minimize the impact of these effects. But most modern communication uses these properties of non-linearity for various reasons. They have come up with fibers that show these effects. HNLF is one such instance.

HNLF is a specifically designed fiber with a higher nonlinear coefficient. The nonlinear coefficient is a measure of the amount of induced non-linearity in a fiber. In general, fibers that are used in optical communication have a nonlinear coefficient of about 1 W-1/km. HNLFs have this value as high as more than 10 W-1/km. Due to this feature of HNLF it is a promising platform for a wide range of applications, such as optical communication and processing, amplification, sensors, meteorology and spectroscope [34].

2.2.3 Optical modulation formats

Modulation is a process of modifying the amplitude, phase or frequency of the high-frequency carrier in accordance with the low-frequency information signal. Modulation formats improve the channel operation to achieve better performance in optical fiber communication. Generally, there are two methods identified for applying electrical modulation into the optical carrier. The first method is directly modulating the source driving current called direct modulation and the second method is modulating the source light by mean of external modulator called external modulation [34–36].

There are different types of modulation schemes such as ASK, FSK, PSK and QAM based on which parameter of the signal is considered in the modulation process.

2.2.3.1 Amplitude shift keying (ASK)

ASK is a digital modulation scheme that modulates the intensity of the carrier [37]. Here, the amplitude of the carrier signal is changed with respect to an information signal. By this method, binary 1 of the information signal is transmitted without a change in the carrier amplitude while binary 0 is transmitted by suppressing the carrier amplitude fully or partially (Figure 2.6) [16, 38].

Simply, the direct modulation method of the laser drive can be used to generate ASK modulation. However, this method incurs problems due to the inability of semiconductor lasers to maintain a stable output frequency with charging drive current. Then the external modulation can be introduced by using directional couplers or the Mach-Zehnder Modulator (MZM) (active integrated optical devices). All external ASK modulator's major drawback is wastage of half of the transmitter power [34, 39].

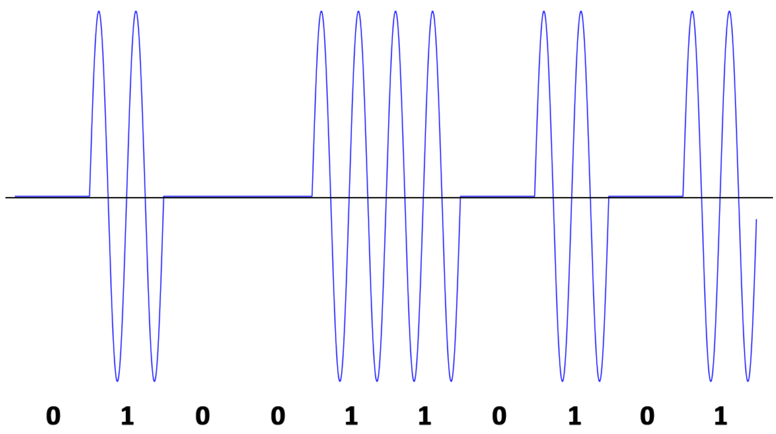

Figure 2.6: ASK modulated signal

2.2.3.2 Frequency shift keying (FSK)

Switching the frequency of the laser light between two frequencies according to the information signal is known as FSK (Figure 2.7). The envelope of optical signals stay unchanged in the FSK modulation technique. The simplicity of producing and receiving the ASK system is better compared to FSK. FSK can also be generated using direct modulation and external modulation [39].

The different FSK modulation formats can be defined by changing the Modulation index. The most simple FSK format is binary FSK (BFSK). In BFSK binary data are transmitted by using two discrete frequencies. The binary "1" is named as the mark frequency and the "0" is named as the space frequency. Multilevel FSK (MFSK) is used to increase the choice of signaling frequencies and it helps to improve the coherent optical receiver sensitivity [40, 41].

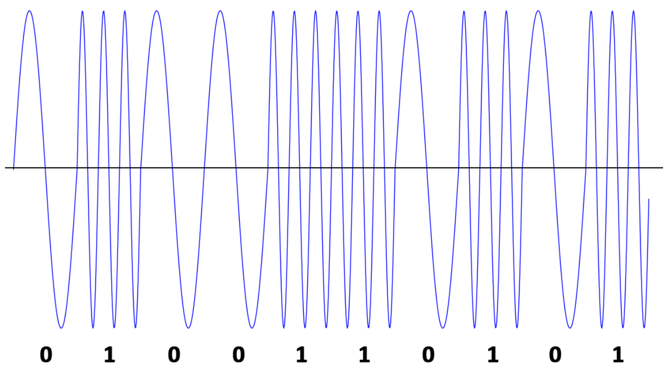

Figure 2.7: FSK modulated signal

2.2.3.3 Phase Shift keying (PSK)

PSK is a digital modulation method that changes the instantaneous phase of the carrier signal according to the information signal (Figure2.8). A constant signal envelope and a narrow spectrum of PSK optical signals have the way to improve the nonlinear tolerance of the system [16]. PSK uses a set of phases that represents a set of unique binary values. The bit count of each of these binary values are same [36, 39, 42]. There are various types of PSK systems. Some of the more frequently used forms are BPSK, differential phase shift keying (DPSK) and quadrature phase shift keying (QPSK).

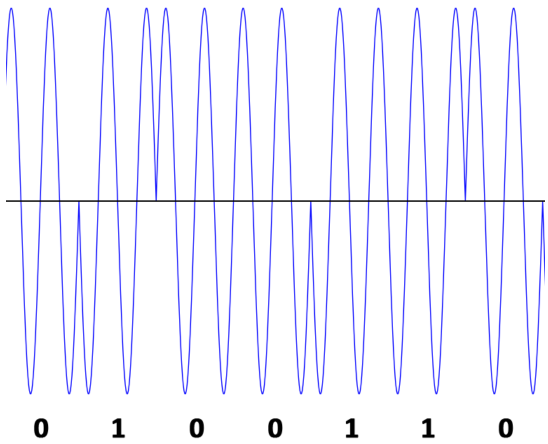

Figure 2.8: PSK modulated signal

- Binary Phase Shift keying (BPSK)

BPSK is the simplest PSK modulation technique. It has one fixed phase when binary 1 is represented and it changes by π when binary 0 is represented. An example waveform of the BPSK signal is illustrated in figure2.9.

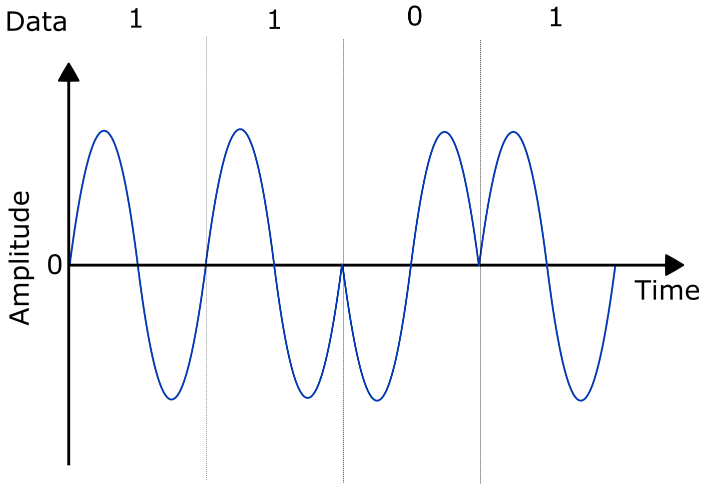

Figure 2.9: BPSK modulated waveform

In this method, the two valid constellation points are placed anywhere on the constellation diagram by separating them with 180° phase difference and figure 2.10 shows that they are at 0° and 180° on the real axis. It is not suitable for high data rate application however it can handle the highest noise level or distortions. [16, 36, 43].

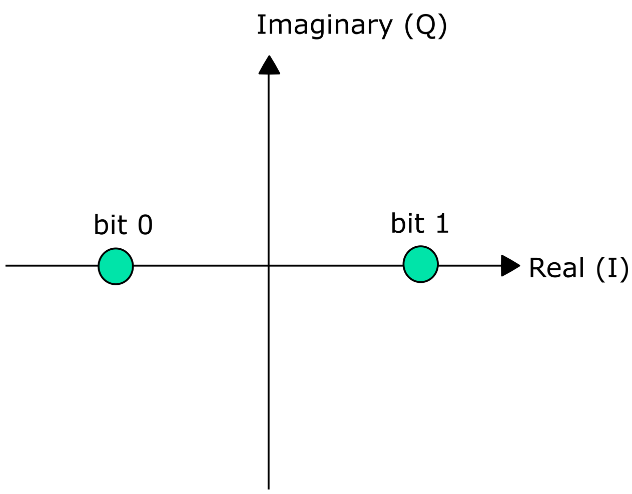

Figure 2.10: BPSK constellation diagram

- Differential Phase Shift keying (DPSK)

DPSK is a different version of BPSK. But it is significantly fairly complicated to implement than BPSK. Because it is a non-coherent scheme, therefore no reference signal is required and the phase of the DPSK modulated signal is shifted relative to the previous bit.

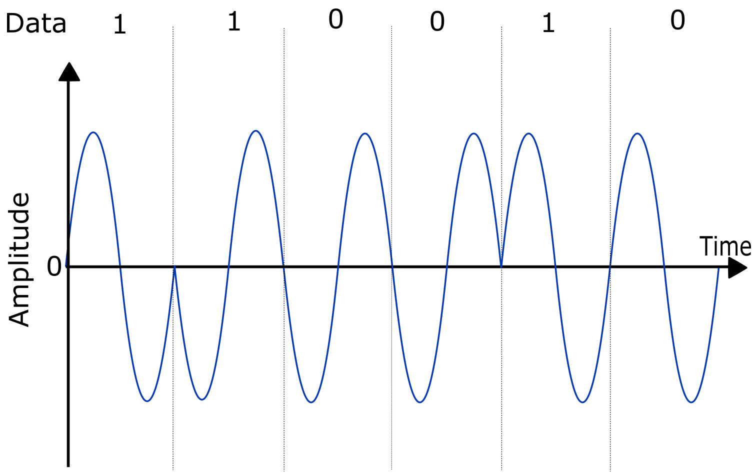

Figure 2.11: DPSK modulated waveform

The following figure2.11 represents the waveform of a DPSK modulated signal. According to the figure, if the next data bit is 1 then the phase of the signal is inverted, but if the next data bit is 0 then the phase of the signal remains unchanged and continues as it was.

As mentioned for the BPSK constellation diagram, phase values 0 and pi are encoded as bit 0 and 1 (figure2.10). [36, 44].

- Quadrature Phase Shift Keying (QPSK)

QPSK is also known as 4-PSK. The constellation diagram for the QPSK signal represented in the figure2.12 includes four constellation points. A single constellation point encoded in two bits (00, 01, 10 or 11).

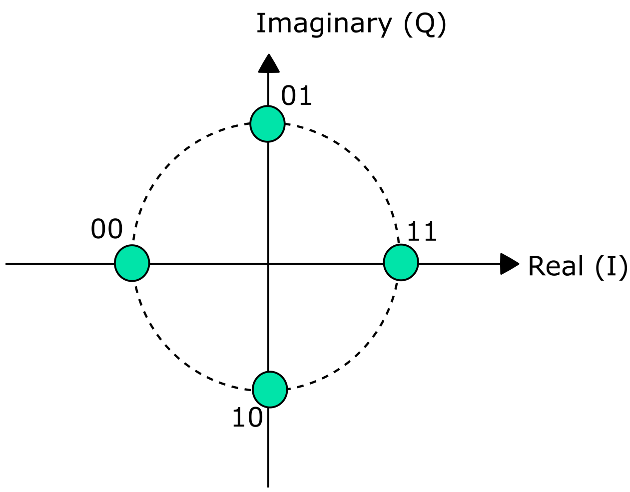

Figure 2.12: QPSK constellation diagram

The figure2.13 shows the QPSK waveform for all four possible combinations of two bits and the maximum phase separation is 90. Compared to the BPSK system QPSK can be used to double the data rate without changing the signal bandwidth [16, 45].

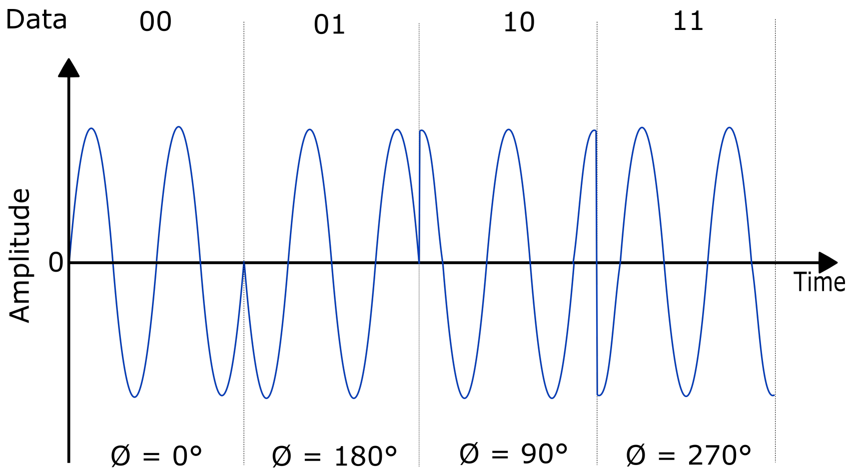

Figure 2.13: QPSK modulated waveform

2.2.4 Linewidth of Laser

Laser linewidth is the width of the emission spectrum of a laser beam. Simply it is the width of the power spectral density of the emitted electric field. Linewidth is measured in terms of frequency, wavenumber or wavelength. Linewidth is often defined in terms of the full width at half maximum (FWHM) of the optical field power spectrum [46]. Fleming and Mooradian, found there is a Lorentzian shape for the signal spectrum and there is an inverse relationship between output power and the FWHM linewidth value [47]. This Laser linewidth can be changed due to the internal and external property of the laser. As an example, it can be changed due to the phase fluctuation of the optical field [48–50] or due to the change of refractive index with carrier density [51, 52].

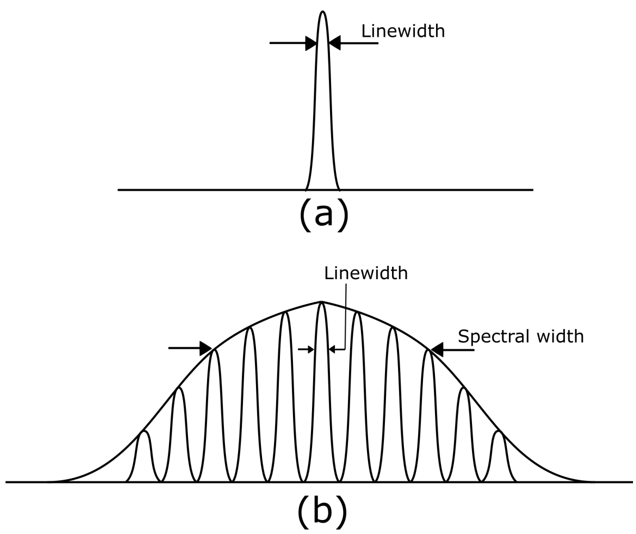

Figure 2.14: (a)Linewidth of a single wavelength (single-mode) laser diode, (b) Linewidth and Spectrum width of a multiple wavelength (multi-mode) laser diode

Figure 2.14 illustrates the concepts of linewidth and spectral width. As shown in the figure linewidth broadening occurs due to the phase noise of the optical carrier. Spectral width is the measurement of the spectral content of the multiple wavelength laser diode. It relates to the envelope of the spectrum and is controlled by the wavelength dependence of the material gain in the laser diode [6, 53].

The Schawlow Townes expression is used to calculate the fundamental value of spectral width [54]. But the fundamental value of a narrow linewidth laser is difficult to measure, because the narrow line laser light will be subject to frequency jitter [55]. Frequency jitter is the random change in the operating frequency of the laser over the time. Usually, it occurs due to pump laser noise, acoustic noise, vibrations, etc. The effect of frequency jitter widens the spectrum. But that effect on the linewidth can be reduced by measuring further down on the displayed spectrum. Therefore, the measured linewidth is then transformed into the correct FWHM linewidth [56].

Practically, the Grating based optical spectrum analyzer cannot be used to measure the laser linewidth because optical spectrum analyzers (OSAs) do not offer the required measurement resolution. Therefore, alternative methods must be used [57–59]. Some of them are,

- Optical heterodyne method
- Delayed self-heterodyne method

- Delayed self-homodyne method
- Optical discriminator technique

Those methods are capable of obtaining the extremely high resolution required for laser linewidth measurements. There are advantages and disadvantages of each method, by understanding those limitations and advantages the best method can be selected to use in particular application [60]. Among those techniques, the delayed self-heterodyne method is known to be the most sensitive method to analyze the laser linewidth.

2.2.5 Laser linewidth measurement methods

Among all the linewidth measurement techniques, the optical heterodyne method can characterize both symmetric and non-symmetric spectral lineshapes. Also, it can be used to identify the optical spectrum of unknown signals. This method has high resolution and sensitivity. As shown in figure 2.15 commonly used optical heterodyne system required the reference laser with a stable, narrow linewidth (local oscillator). The light from the local oscillator is combined with the signal laser using a coupler and there is a polarization state converter in the local oscillator path. Then the output signal is divided into two ports using a power splitter. One port leads to an OSA and the other one leads to an electrical spectrum analyzer (ESA) [55, 61].

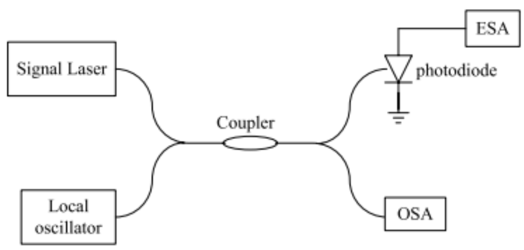

Figure 2.15: Schematic of the setup for optical heterodyne detection

The ESA output spectrum displays the combination of direct detection and heterodyne spectrum [57].

$$S_i(f) = R^2[S_d(f) + 2(S_{LO}(\nu) \circledast S_s(-\nu))] \tag{2.1}$$

Where, R - Detector responsivity
$S_d(f)$ - Ordinary detection

$S_{LO}\nu$ - Local oscillator spectrum

S_ν - Signal spectrum

$S_{LO}(\nu)$ is approximated with Dirac delta function $P_{lo}(\nu - \nu_{lo})$, when local oscillator laser linewidth is small compared to the signal laser linewidth. Thus the spectrum display in ESA can write as a,

$$S_i(f) = 2R^2 P_{LO} S_s(\nu - \nu_{LO}) \tag{2.2}$$

Where, P_{LO} is the power of local oscillator

The delayed self heterodyne method also has a similar technique as the optical heterodyne method. But a separate local oscillator laser is not necessary here. This concept is briefly shown in figure 2.16 2.16 [3].

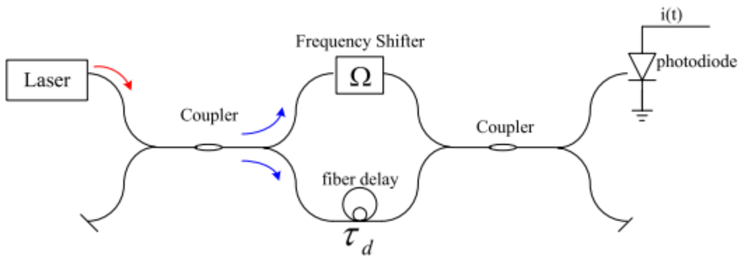

Figure 2.16: Schematic of the setup for optical delayed self-heterodyne detection [3]

As shown in the figure the laser light is split into two paths by the interferometer and one arm is delayed with respect to the other arm which contains a frequency shifter. Variety of devices can be used as frequency shifters such as acousto-optic frequency shifter, phase modulator and intensity modulators.

If the delay time of the laser is higher than the coherent time, the two combined beams are considered as they were generated from two separate lasers. Therefore, the system performs similarly to the optical heterodyne method. Here the ESA spectrum is a convolution of the individual power spectrum of the interfering waves [57].

$$S_i(f) = R^2[S_d(f) + 2(S_s(\nu - \delta\nu) \circledast S_s(-\nu))] \tag{2.3}$$

Where, $\delta\nu$ is the shift frequency

The displayed FWHM lineshape will be twice the actual lineshape of the Lorentzian shape spectrum and it is larger by a factor of $\sqrt{2}$ than the actual lineshape of a Gaussian shape [62]. The ESA displayed lineshape is always symmetric even if the original lineshape is asymmetrical because the spectrum is convoluted with itself [57]. For this reason in this research, delayed self-heterodyne method is used as the linewidth measuring technique.

2.2.6 Phase synchronization

Synchronization is a process of equalizing the appearance of two different signals due to the interaction. Phase synchronization is a process of two or more signals that tend to oscillate with a repeating sequence of relative phase signal. It is usually defined as locking of the phase [63].

Therefore if the relative phase is a constant, it is assumed to be the phase of the interactive waves are locked to each other. In equation 2.14 gives a relationship considering two signal phases but this can be extended to multiple signals,

$$\Delta\Phi = n\Phi_1 - m\Phi_2 = C \tag{2.4}$$

Where,
$n\Phi_1$ is the phase of the reference signal
$m\Phi_2$ is the phase of the 2nd signal
m, n integers, while C is a constant

The phase difference of two signals is a constant value [64]. Over the years, different phase synchronization methods have been developed and implemented.

- Optical Phase Locked Loop (OPLL)

An OPLL is a control system that generates an output signal with a phase equal to or in a constant relationship with the phase of the input signal.

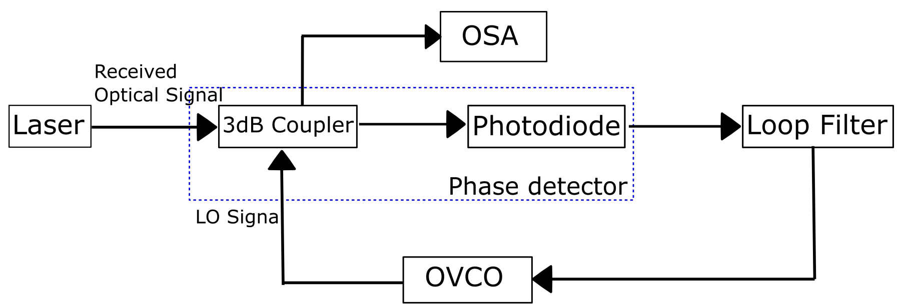

Figure 2.17: Block diagram of OPLL

The figure 2.17 shows the fundamental configuration of OPLL. This architecture mainly consists of a phase detector, a loop filter and an optical voltage controlled oscillator (OVCO). The phase detector is used to generate an error signal which is proportional to the phase difference between two signals. Both received optical signal and local oscillator (LO) are combined using a 3dB directional coupler. And Photodiode (PD)is used to convert the optical signal to electrical domain [65]. The loop filter is used to filter the phase error signal to operate the OVCO. An optical continuous wave (CW) signal was generated by OVCO and the frequency of the signal depends on the input voltage [66, 67].

- Optical Injection locking (OIL)

Optical injection locking is a technique which is used to operate a laser (slave laser) on a certain frequency by injecting external light (master laser) with that particular frequency. This is a technique used to achieve the synchronization in-terms of both laser frequency and phase. Optical injection locking system produces the enhancement of performance against the free running laser. It can be used to improve side mode suppression [68], enhance bandwidth, relaxation of oscillation frequency [69], suppressing of nonlinear distortion and reducing the relative intensity noise [4, 70, 71].
Figure 2.18 shows the two possible methods for injection locking a salve laser [4].

- Transmission style
- Reflection style

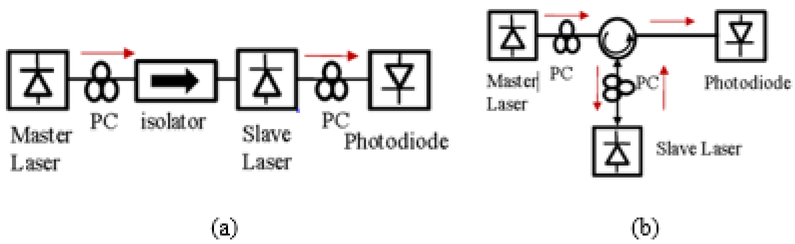

Figure 2.18: Schematic diagram of optical injection locked laser system (a) Transmission style (b) Reflection style [4]

During the injection locking, the slave laser wavelength and phase is locked to the master laser wavelength and phase. In transmission style, the injected master laser light is entered through one facet of slave laser and the output is taken from the other facet. The isolator is used to avoid the back reflection being fed to the master laser. Transmission style setup can be easily converted into the reflection style setup. In this style, same slave laser facet is used to inject the injected master laser light and to take the output. The optical circulator is used to obtain only the injection locked output of the system. In both systems, polarization controllers are used to match a master and slave polarization [4, 72, 73].

The main requirement to achieve phase synchronization using OIL and OPLL a carrier should be available with signal. Exploiting the phase information and achieving phase synchronization through OIL or OPLL from carrier less, noise contained signal slightly difficult and complicated. In this thesis use carrier less BPSK modulated signal for carrier recovery therefore, it uses the nonlinear technique of FWM to recover the phase information of the input carrier from the BPSK modulated signal.

2.2.7 Nonlinear Phenomenon

In an optical fiber, a nonlinear effect occurs due to the changes of the core medium refractive index with an optical intensity and inelastic scattering phenomenon. Kerr nonlinearity effect was generated due to the dependence of the refractive index on the optical power. Nonlinear optics started as a growing research area after the second harmonic generation [74] by Franken and his team [75]. Nonlinear effects can be mainly divided into two categories [76].

1. Effects depend due to the refractive index on the optical power - Kerr effect
2. Effects due to the interaction of phonons in fiber medium with lightwave - Inelastic scattering

Effects due to the dependence of refractive index on the optical power:

1. Four wave Mixing (FWM)
2. Self-Phase Modulation (SPM)
3. Cross Phase Modulation (XPM)

Effects due to the interaction of phonons in fiber medium with lightwave:

1. Raman Scattering
2. Brillouin Scattering

All nonlinear effects depend on and are proportional to the link length and the cross section of the fiber. Except SPM and XPM, all other nonlinear effects provide gain to some channels. SPM and XPM effects only the phase of the signal and it can cause increased dispersion and that cause the spectral broadening [77,78]. Attenuation in fiber too participates in the process of reducing the signal being propagated. So the following equation gives an approximate value of the effective length in modelling fiber systems [76]:

$$Le = \frac{1 - e^{-\alpha L}}{\alpha} \tag{2.5}$$

Where, Le is the effective length, L is the length of the fiber and α is the attenuation coefficient in m^{-1}. In conventional SMF, the attenuation can be low value (0.16 - 0.2 dB/km) and typical HNLFs attenuation is around 0.8 -1.2 dB/km. The total attenuation is reduced with the implementation of nonlinear devices in HNLF due to the low length of fiber.

2.2.7.1 Four Wave Mixing

A main nonlinear phenomenon that is arising from 3rd order susceptibility which is a result of the Kerr effect of silica fiber. It occurs when at least high power two different frequency components propagate together in a nonlinear medium. The new signals generated by mixing the original signal which is propagated to the output are called FWM products or idlers [79–81].

The number of new idlers can be calculated using,

For N number of signals

$$Number\ of\ new\ Idlers = N^2/2(N-1) \tag{2.6}$$

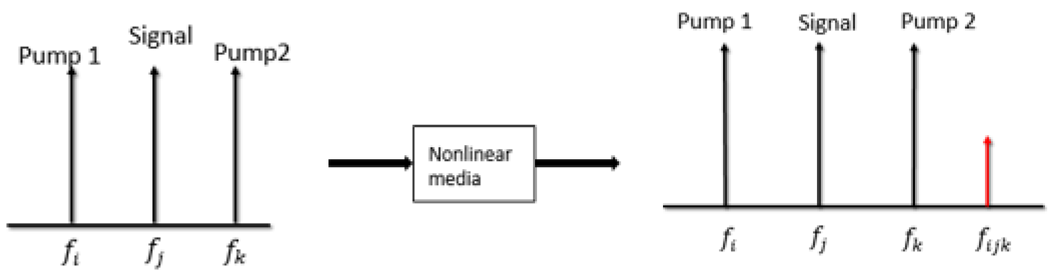

Figure 2.19: Non-degenerate Four Wave Mixing

Four wave mixing can be categorized into two types according to the number of frequencies involved at the input:

- Non-degenerate .
- Degenerate .

Figure 2.19 shows four wave mixing in frequency domain using three different signals. The frequency f_{ijk} and the phase Φ_{ijk} of the FWM products are given by,

$$f_{ijk} = f_i \pm f_j \pm f_k \tag{2.7}$$

$$\Phi_{ijk} = \Phi_i \pm \Phi_j \pm \Phi_k \tag{2.8}$$

Where,
f_i, f_j, f_k – frequencies of the interacting signals
Φ_i, Φ_j, Φ_k - phases of the interacting signals

If waves are distinct $(i \neq j \neq k)$ the FWM process is called the non-degenerate FWM. If the two waves are identical $(i = j \neq k$ or $i \neq j = k)$ the FWM process is called the degenerate FWM.

This degenerate FWM process generate significant two idler waves [34, 35, 82]

$$E_{i1} = E_s^2 \cdot E_p \cdot e^{(i((2\omega_s - \omega_p)t - (2\Phi_s - \Phi_p)))} \tag{2.9}$$

$$E_{i2} = E_p^2 \cdot E_s \cdot e^{(i((2\omega_p - \omega_s)t - (2\Phi_p - \Phi_s)))} \tag{2.10}$$

Where,

E_{i1} - electric field variation or the amplitude of new idler closer to the signal

E_{i2} - electric field variation or the amplitude of new idler closer to the pump

E_s, E_p - signal and pump field strength

ω_s, ω_p – signal and pump angular frequencies

Φ_p, Φ_s – signal and pump phases

The frequency and phase of new idler closer to the signal and pump can be written as,

Frequency of new idlers, [34, 35, 82]

$$f_{i1} = 2f_s - f_p \tag{2.11}$$

$$f_{i2} = 2f_p - f_s \tag{2.12}$$

Phase of new idlers, [34, 35, 82]

$$\Phi_{i1} = 2\Phi_s - \Phi_p \tag{2.13}$$

$$\Phi_{i2} = 2\Phi_p - \Phi_s \tag{2.14}$$

Where,

f_{i1} - frequency of new idler closer to the signal
f_{i2} - frequency of new idler closer to the pump
f_s, Φ_s - frequency , phase of the signal
f_p, Φ_p - frequency , phase of the pump

By considering the equations 2.12 and 2.13, we can see that one idler phase can be used to erase the data which is modulated in the optical carrier at the transmitter. If equation 2.12 is considered, for each signal phase "0", the idler 1 phase contribution is always "0" and for each signal phase "π", the idler 1 phase contribution is "2π", which is equivalent to "0". Thus if a BPSK data signal is considered ("0" and "π" phase) it is noticed both phases have been erased. This is illustrated in table 2.1.

Table 2.1: Idler phases for different data phases

Pump Phase	**Signal Phase**	**Idler 1 (at f_{i1})**	**Idler 2(at f_{i2})**
0	0	0	0
0	π	$2\pi = 0$	$-\pi$

Therefore, it can be concluded that the phase modulation has been stripped from the idler 1 and it tracks the phase of the signal and pump [16, 83].

2.2.8 Optical signal to noise ratio (OSNR)

The optical fiber is an essential measurement technique in the optical communication system. The performance of the optical fiber can be validated through the fiber loss parameters. There are two main loss mechanisms that are generated inside the fiber due to the material absorption and Rayleigh scattering. Material absorption is an intrinsic property of material that may cause some attenuation in the signal as it propagates along the fiber. Currently, the fibers have an attenuation of around 2.5, 0.4, and 0.2 dB/km in 0.8μm, 1.3μm and 1.5μm wavelength bands respectively which are used in optical communication [84, 85]. The most significant loss is the scattering loss due to the Rayleigh scattering. Due to the losses, after substantial propagation distance, the signal power will be reduced below the detectable threshold of optical receivers. Therefore, communication systems require optical amplification. The main impact of optical amplification is the generation of ASE [86].

Optical amplifiers do not only amplify the signal power, but also add noise power which will result in reducing signal performance at the receiver. Therefore, OSNR is an important measure of the performance of any long-distance communication system. OSNR is typically defined as the ratio of the average optical signal power to the total optical noise power measured at the signal bandwidth.

$$OSNR = \frac{\text{Optical Signal Power}}{\text{Optical Noise Power measured at the signal bandwidth}} \tag{2.15}$$

Since this is a ratio between two powers, the output is a dimensionless unit. It is often given in decibels. The OSNR value has a direct relationship with the Q-factor and Bit Error Rate (BER) value [87]. BER is the parameter that is used to determine the quality of the received bit at the receiver.

This OSNR value drops due to the impairments in the transmission path. Generally, an external OSNR setup added to the signal path using a tap coupler for analyzing the signal variation with the OSNR. In this research the linewidth variation of the recovered carrier was measured with the variation of the OSNR. [88, 89].

2.2.9 Dispersion

Dispersion phenomenon is the light pulse broadening when they travel along the optical fiber [16]. This is mainly due to the wavelength dependent refractive index of the silica fiber. It causes distortion for both digital and analog transmission. The dispersion phenomenon which is generated in the digital transmission is presented in figure 2.20. As shown in the figure, indistinguishable pulses can be observed at the receiver point due to the pulse broadening and overlapping with neighboring pulses. The number of errors occur in the digital optical channel is increasing due to this effect which is named "inter symbol interference (ISI)" [8, 90, 91].

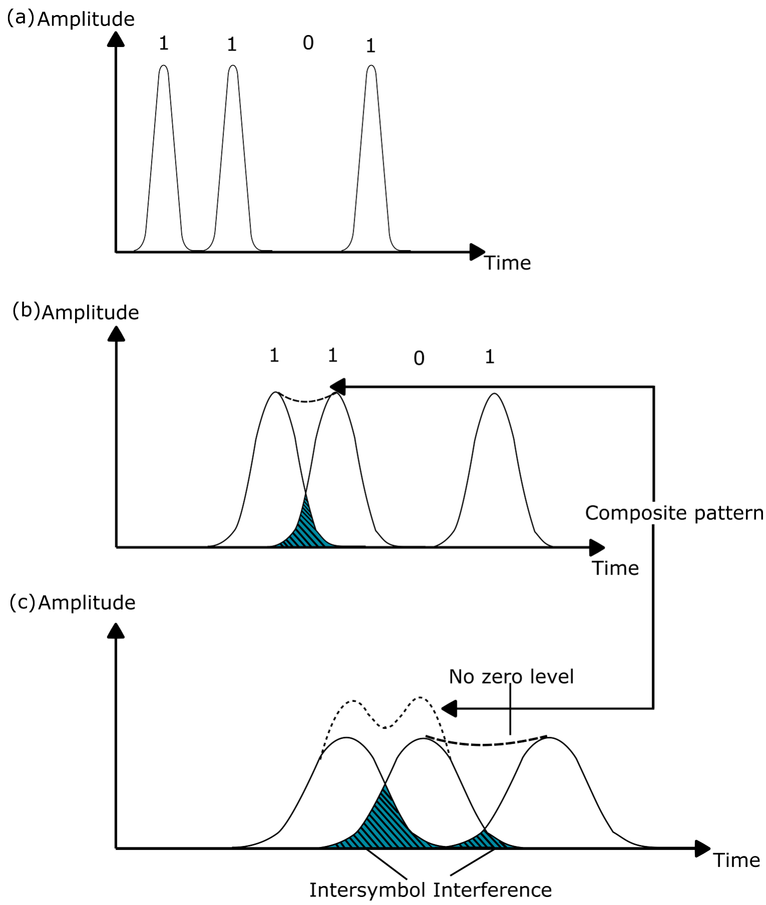

Figure 2.20: The broadening of light pulses when they are transmitted along a fiber for digital bit pattern 1101: (a) fiber input; (b) fiber output after L1 distance; (c) fiber output after L2 distance (L2 > L1)

However, the dispersion can distort the signal such that the individual symbols can no longer be distinguished and this limits the bandwidth of the particular optical fiber.

Figure 2.21 diagrammatically illustrating the pulse broadening associated with the multimode step index, multimode graded index and single-mode step index fibers which are the three main optical fiber structures. As observed from the figure, the lowest pulse broadening given from the single mode fiber and the multimode graded index fiber has lower dispersion than the dispersion of multimode step index fiber. A single mode fiber is has the highest transmission band-

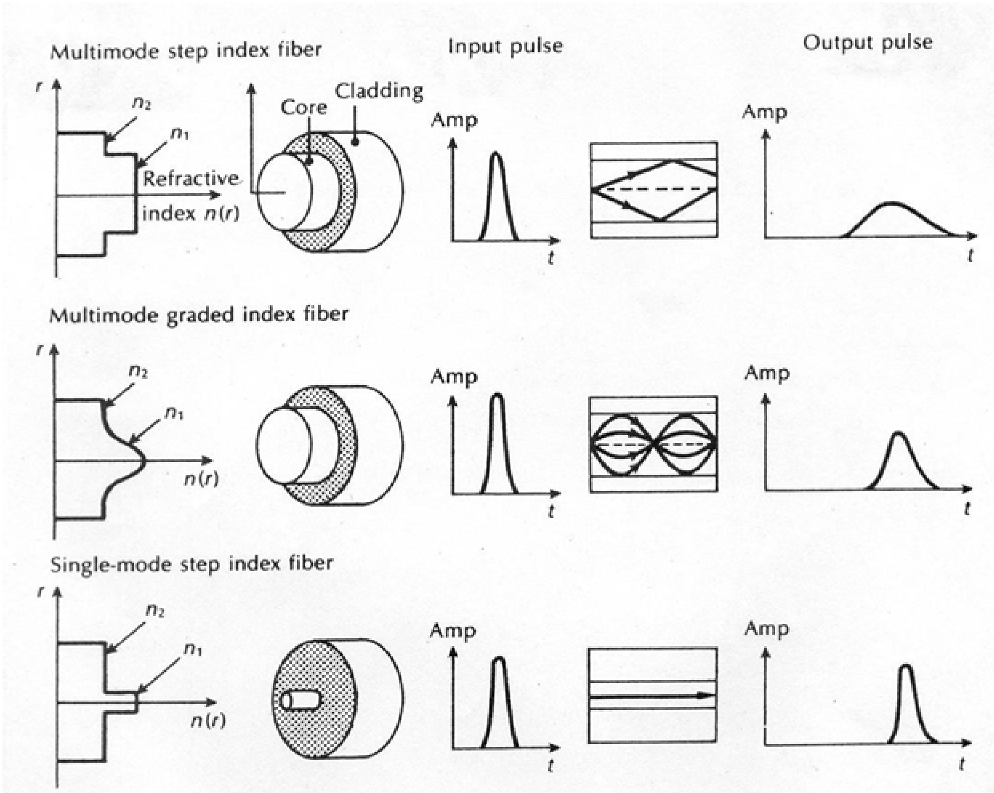

Figure 2.21: Pulse broadening in a multimode step index fiber, multimode graded index fiber and single-mode step index fiber due to the intermodal dispersion. [5]

width which is in gigahertz range and multimode fibers are limited to megahertz range [8, 92].

The amount of pulse broadening is increased with the pulse travel distance through the optical fiber. The light pulse should be detected before it is reconstituted. Therefore, there are some restrictions on usable bandwidth of each fiber link and bandwidth is detected by the distance between the regenerative repeaters. Thus, the pulse broadening in time for a unit length of fiber states as the dispersive properties of a particular fiber. Hence, the information carrying capacity of the fiber is limited by the amount of pulse broadening in unit length. The bandwidth is inversely proportional to fiber distance due to the pulse broadening increases with fiber length. Figure 2.21 shows the typically best bandwidth-length product for multimode step index (20MHz km), multimode graded index (1 GHz km) and single-mode step index (100 GHz km) fibers [8, 93].

2.2.9.1 Chromatic Dispersion

Chromatic or intramodal dispersion occurs due to the spreading of the spectral modes in all types of optical fibers and the dispersion is directly proportional to the spectral width of the source [39, 42]. Since the optical sources are normally emitted a band of frequencies instead of emitting single frequency, there is a delay between propagation of the different spectral components of the transmitted signal. This enhances the intramodal dispersion by broadening each transmitted mode. Intramodal dispersion is considered as an important loss factor in single mode fibers [94]. The loss that occurs due to the intramodal dispersion in a multimode fiber is negligible when considering the other losses in multimode fibers but it is a great concern when considered in the single mode fiber [91, 95, 96].

Intramodal dispersion can be given by the equation:

$$\sigma = \sigma_s \times D_m \times L \tag{2.16}$$

Where, L is the fiber length, D_m is the Dispersion coefficient in ps/nm/km and σ_s is the spectral width [8].

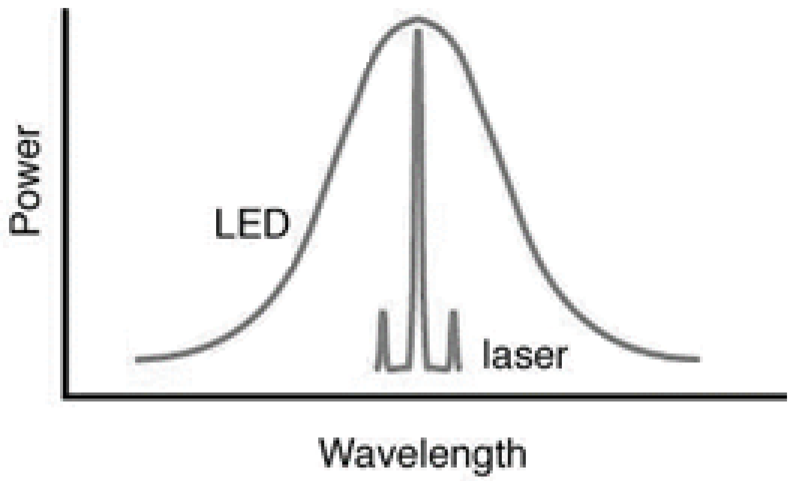

Figure 2.22: LED and LASER spectral broadening

As shown in figure2.22, the LED will cause more Intramodal dispersion than the laser and it has a larger spectral width than a laser, because the injection laser corresponds to only a fraction of a percent of the center frequency. But for the LED, it is a significant percentage. Chromatic dispersion is a combined effect of both waveguide and material dispersion [16].

- Material dispersion

Material Dispersion is caused due to atomic structure of the material; mainly because of different elements being present in the fiber material during the manufacturing process. The pulse broadening due to the material dispersion is generated because each wavelength component of an initial pulse passes with unequal group velocities. Laser pulses are almost monochromatic and consist of many wavelengths in a small range. Normally, the refractive index of a material depends on the wavelength. Therefore each frequency component has a different speed. The pulse becomes broadened with the increase of distance and the material dispersion limits the data capacity [76, 97, 98] .

- Waveguide dispersion

  Waveguide dispersion depends on the propagation characteristics where the propagation characteristics depend on the angle that a ray hits the cladding. Therefore, the dispersion occurring in this particular method strictly depends on the refractive index of the core, the cladding of the fiber and the wavelength of the source. In multimode fiber, waveguide dispersion is negligible when compared to material dispersion because the majority of modes propagate far from cutoff. But when it comes to single mode fibers it is considerable [76, 98].

2.2.9.2 Intermodal dispersion

Pulse broadening due to intermodal dispersion is a result of the propagation delay differences between modes. Intermodal Dispersion takes place in step-index multimode fibers where the core diameter usually is around 62.5 μm [8]. The pulse width of the output signal is depending on the receiver time of the slowest and fastest modes because, different modes pases through the fiber at different group velocities [99].

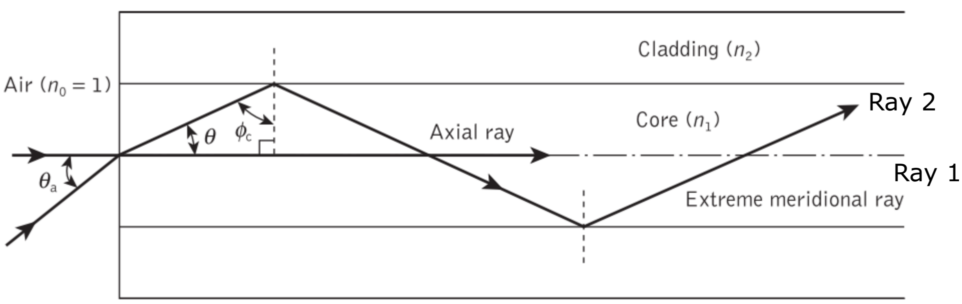

Figure 2.23: Light ray propagation in fiber

Figure 2.23 shows the differences of the delays of two rays passing through the fiber core. When both rays are travelling at the similar speeds within the constant refractive index, the differences of the delays directly depends on their path length. Here, Ray 1 (Axial ray) is the ray that travels straight through the core and it is the fastest at the receiver end. Ray 2 is the ray that makes the critical angle with the cladding and it arrives last at the receiver end. All other rays arrive in time between the arrival of these two rays. Equation 2.17 will give the time delay between the critical angle ray and the axial ray. Large amount of intermodal dispersion will lead to ISI which might cause a tendency of bit errors.

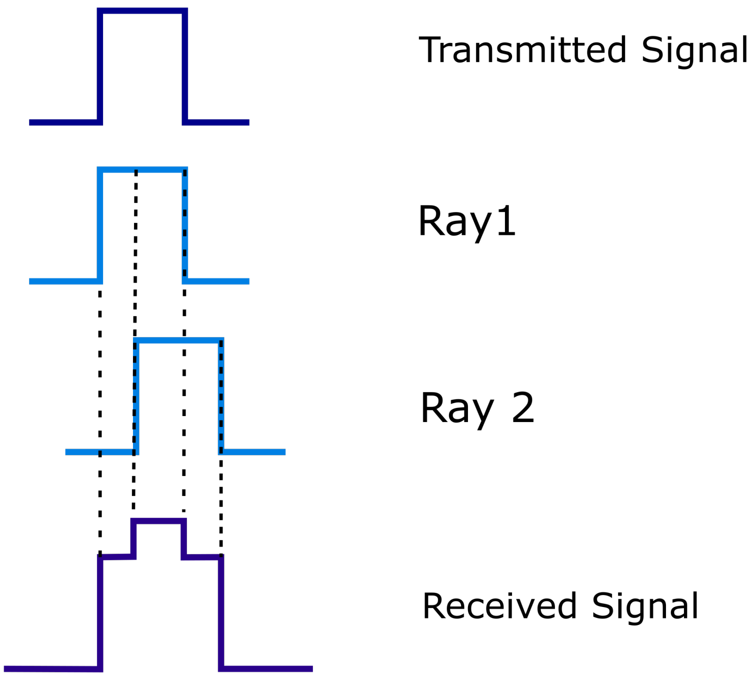

Figure 2.24: Rays traveling at different velocities

Intermodal dispersion can be given by the following equation:

$$\Delta t = (L\frac{n_1}{C})(\frac{n_1}{n_2} - 1) \qquad (2.17)$$

Where n_1 is a refractive index of core, n_2 is a refractive index of cladding and C is the velocity of light in a vacuum [100].

2.3 Related previous research

In previous studies, researchers investigated various techniques for carrier recovery in optical contexts. Ezra Ip and Joseph M. Kahn show the Electric feed-forward carrier recovery method in their published work, "Feedforward Carrier Recovery for Coherent Optical Communications" [75]. As shown in figure 2.25, the received optical signal is combined with a local oscillator laser using two 90° hybrids and a polarization beam splitter. The outputs of the balanced photo-detectors are the base-band electrical signals. These signals sent through low pass filter and sampled using analog-to-digital converters (ADCs) with high sampling rates. The incoming signals are multiplied using the numerical oscillator. The soft decision phase estimator is used for soft estimating the carrier phase for each signal period. The soft decision estimated phase will acquire an offset equal to the angular difference between the detected signal and the actual signal. In the next stage, the phase estimated signal is passed through a linear filter. The feedback section has a similar structure to a PLL. The major implementation issues of this research are the resolution or the bit count of the ADC and system complexity.

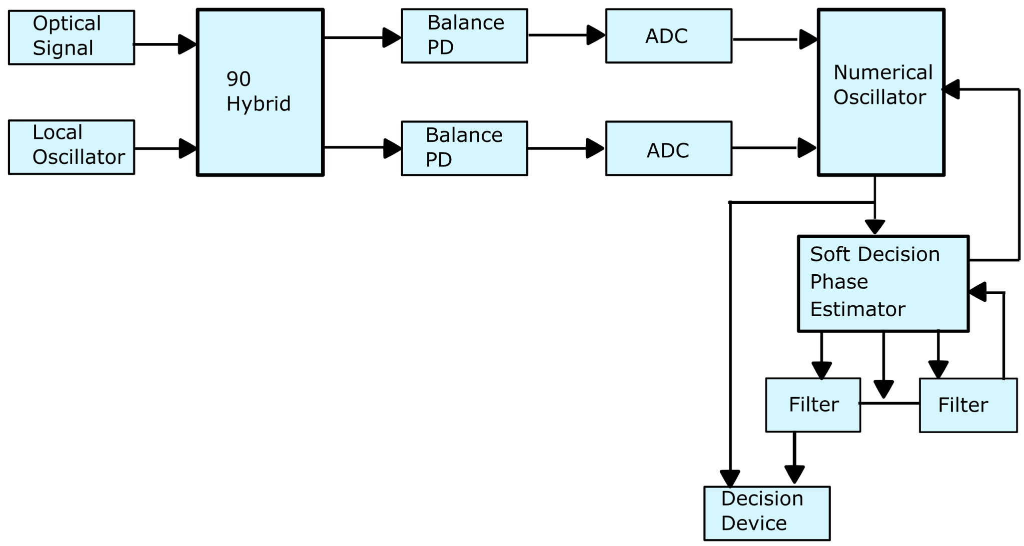

Figure 2.25: Electric feed-forward carrier recovery diagram

A quite similar method presented by Selwan K. Ibrahim, et.al in their published work, "Novel Carrier Extraction Scheme for Phase Modulated Signals Using Feed-Forward Based Modulation Stripping". As illustrated in figure 2.26 this technique uses an Optical-Electrical-Optical (OEO) DPSK re-generator to recover a carrier from a BPSK signal. It is formed in a feed-forward manner by modulating it with a complementary data pattern [101]. This technique can be used to enable optical injection locking and phase lock loop systems for carrier less BPSK signals.

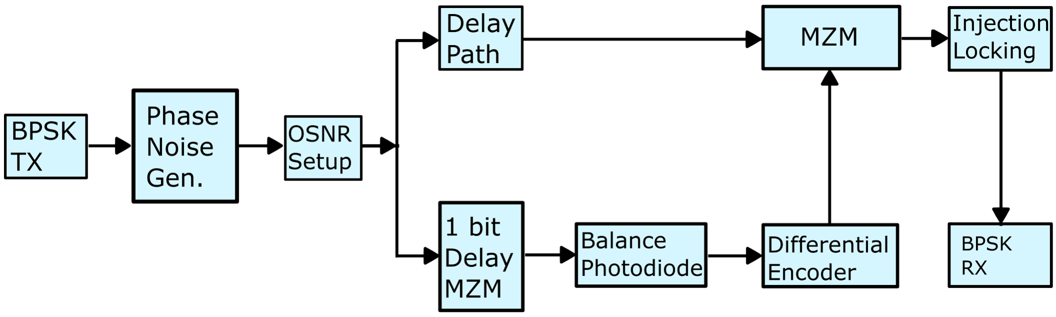

Figure 2.26: Feed-forward based modulation stripping carrier recovery diagram

Another similar study presented by K.T. Wu and H. Sun in their published work, "Techniques in Carrier Recovery for Optical Coherent Systems" [102]. They use feedback and a feedforward carrier recovery method using phase locked loops. These systems include phase locked loops and phase detectors for their efficient carrier recovery. These methods have opted for differential encoding to optimize the outputs. The straight forward phase recovery techniques, including PLL and IL cannot be directly applied for the carrier recovery from the carrier less signal [103]. Then, a new technique was introduced using decision driven PLL for carrier phase recovery [104]. But decision driven PLL technique is difficult to use for practical purposes due to its high bandwidth requirements [105]. As another solution a digital feed forward technique has been introduced for carrier phase estimation [106]. However, both techniques required a polarization alignment.

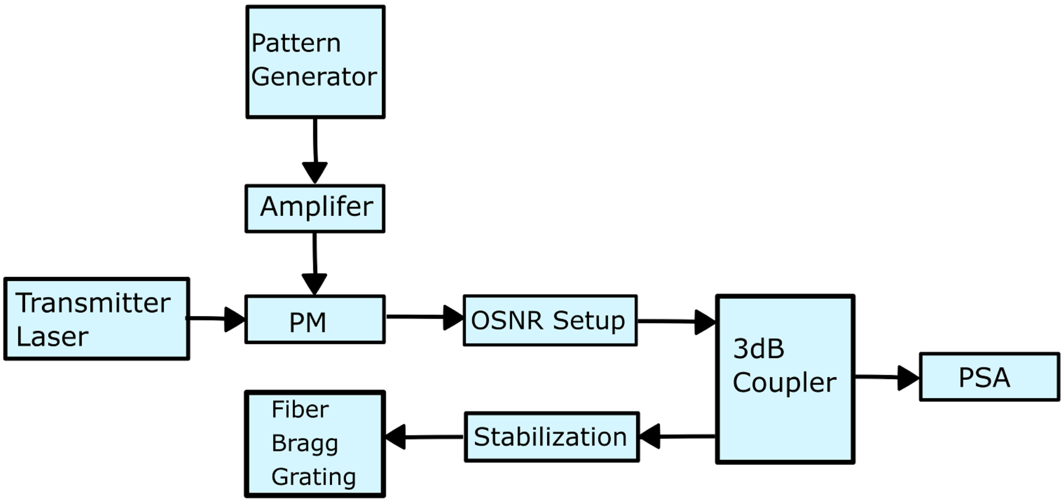

Figure 2.27: Optical phase sensitive oscillator method diagram for carrier recovery

The next new method was introduced by Inwoong Kim, et.al in "All-Optical Carrier Phase and Polarization Recovery Using a Phase-Sensitive Oscillator" [107]. As shown in figure 2.27 this method is used to recover the carrier from the BPSK modulated signal using a PSK data-pumped phase-sensitive oscillator. The phase sensitive oscillator is an optical parametric oscillator with phase sensitive amplifier (PSA) as a gain block. A Nonlinear Mach-Zehnder Interferometer (NMZI) or a Nonlinear Optical Loop Mirror (NOLM) configuration was used as the PSA [108].

The Major issue with this method is the losses. The extinction ratio of the NOLM was limited by a relatively high return loss (17dB) and the total insertion loss. The coupling losses at both ends of the Bi-HNLF were not symmetric. Due to the coupling losses data leaks into the oscillator. The round-trip phase matching condition for the oscillating signal was mainly interrupted by pump frequency noise. It affects more for the long round-trip delay [107].

Meng Qiu, et.al presented a method that can do carrier phase recovery by parallelizing a phase recovery system in "Simple and Efficient Frequency Offset Tracking and Carrier Phase Recovery Algorithms in Single Carrier Transmission Systems" [109]. This paper presents an efficient algorithm that can work as a frequency offset estimator working parallel and sharing these offset information with more parallel streams. Therefore, the frequency offset tracking and carrier phase recovery can be made simpler. The publication titled "Hardware Efficient

Carrier Recovery Algorithms for Single Carrier QAM Systems" was presented by Xiang Zhou [110]. In this research, the blind phase search method is used for single carrier quadrature amplitude modulation (QAM) systems and phase estimation techniques have been used at multiple levels for further improvement of the carrier recovery process.

In previous studies, similar carrier recovery methods have come up with a FWM technique. Cheng Cheng, et al. shows a method to measure carrier recovery time in semiconductor optical amplifiers (SOA) based on dual pump FWM in the publication "Measurement of the carrier recovery time in SOA based on Dual Pump FWM" [11, 111]. This also uses a practical experimental setup as shown in figure 2.28. The injected current has been varied and carrier recovery time has been observed. For example, in the case of 120 mA current, carrier recovery time has been reported as 91 ps.

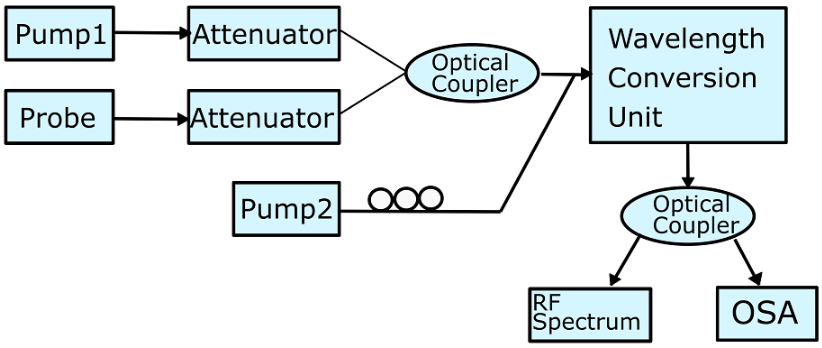

Figure 2.28: Experimental setup of the measurement for the carrier recovery using SOA

Another related study was done by Guo-Wei Lu, et.al and presented in the publication "Format Conversion of Optical Multilevel Signals Using FWM-Based Optical Phase Erasure" [112]. In this research, optical phase deletion has been shown using FWM technique for DPSK systems. They too have used a practical approach to come up with this conclusion.

The foundation of this research taken from the publication "Generation of frequency symmetric signals from a BPSK input for phase sensitive amplification" published by Ruwan Weerasuriya, et al [113]. In this research also a BPSK modulated signal is launched into an actual HNLF to participate in a FWM process thereby recovering the carrier of the modulated signal. This signal is further sent to injection lock a laser to create a frequency symmetric signal for applications using phase-sensitive amplification. Phase sensitive amplification is a phase amplifying process that takes the signal phase to a considerable level when it is applying. At present, phase sensitive amplification is useful for long distance optical communications due to low noise.

All the above research shows techniques for carrier recovery. The majority of them use hardware solutions. Carrier recovery, however, can change as the data levels go up and the fiber material changes. A very recent paper shows how carrier dynamics vary with the frequency especially at TeraHertz level communications and their dependency on the fiber material [114]. Finding a flexible and independent solution is therefore important. In my thesis and research, I have tried to show a system without hardware constraints that can perform carrier recovery. Also, I have further analysed the system and tried to identify the limiting factors for each characterization which is useful in the implementation of this system.

Chapter 3

OPTICAL CARRIER RECOVERY SCHEME

The requirement for carrier recovery schemes arose when the communication systems started transmitting carrier less modulation format, such as phase encoded data format. This research used suppressed carrier BPSK modulated data signal for the analysis of carrier recovery.

The simulation tasks of this research were done using VPItransmissionMaker^{TM} Optical Systems software. Carrier extraction simulation is initially carried out for BPSK signal, the very basic form of PSK. A BPSK transmitter was designed because of the unavailability of an inbuilt BPSK modulator in VPItransmissionMaker^{TM} software.

The schematic diagram of BPSK transmitter was presented in the figure 3.1.

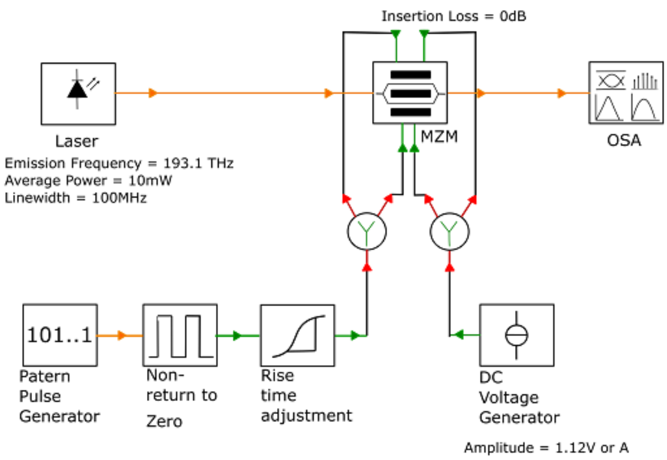

Figure 3.1: The schematic diagram of BPSK transmitter

The BPSK modulated signal was produced by using a random incoming data sequence. A 10 Gbit/s BPSK signal (193.1 THz) was generated with a DFB laser (LW = 100 MHz) and MZM modulator is driven by a pseudo random bit sequence (PRBS) electrical signal from a pattern generator with a 1024 (PRBS 10) pattern length.

Figure 3.2 denotes the output spectrum of BPSK modulated signal which is used to recover the carrier information after transmission, while figure 3.3 denotes the waveform diagram of the BPSK modulated signal.

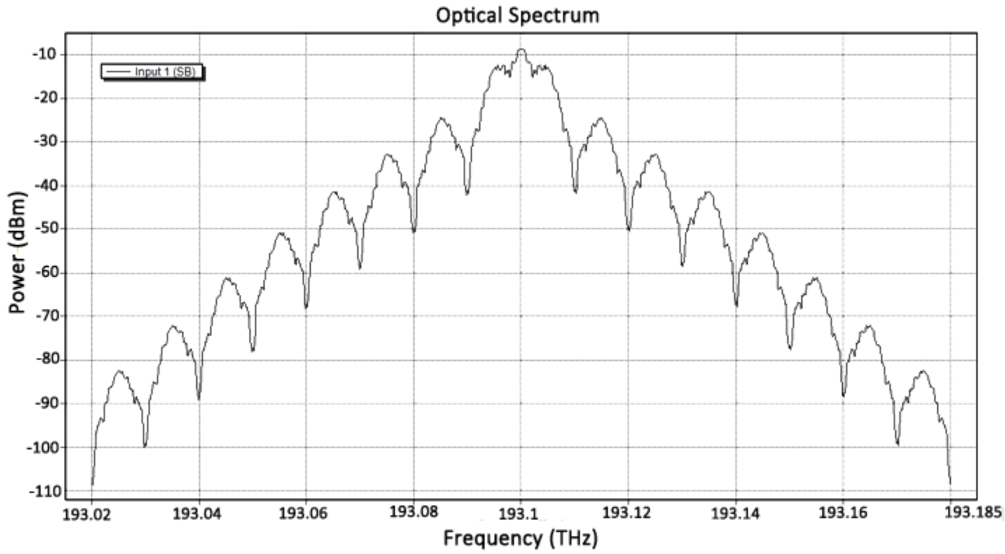

Figure 3.2: Spectrum diagram of BPSK modulated output in frequency domain

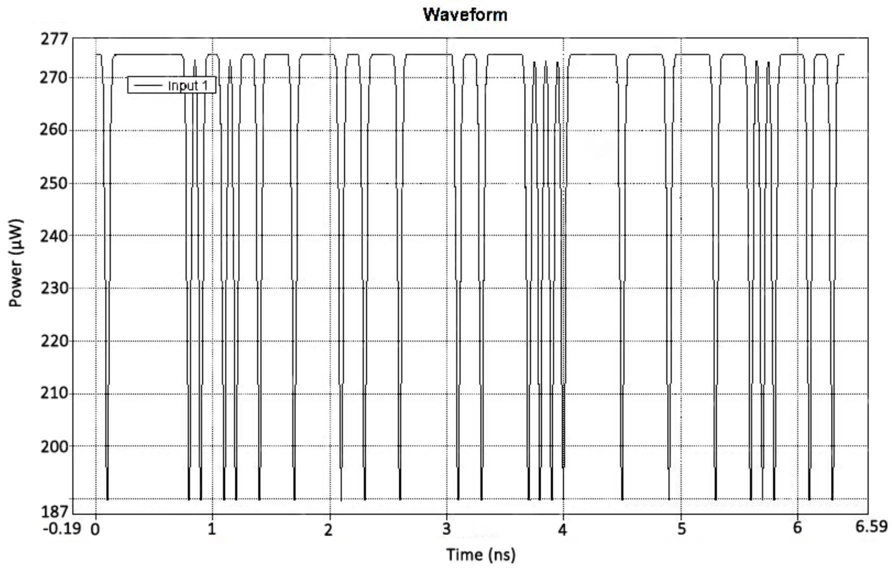

Figure 3.3: Waveform diagram of BPSK modulated output in Time domain

To analyze a phase modulated system, one of the best parameters is to draw the constellation of the transmitted symbols. Therefore, the constellation analysis was carried out and tested for the implemented transmission format to validate the simulated system.

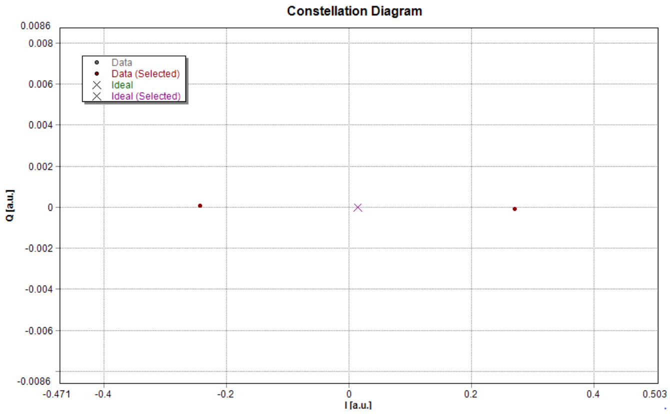

Figure 3.4: Constellation Diagram of BPSK modulated signal

The simulation setup for carrier information extraction from a BPSK modulated signal using FWM in a highly non-linear fiber is illustrated in figure 3.5 [13, 115].

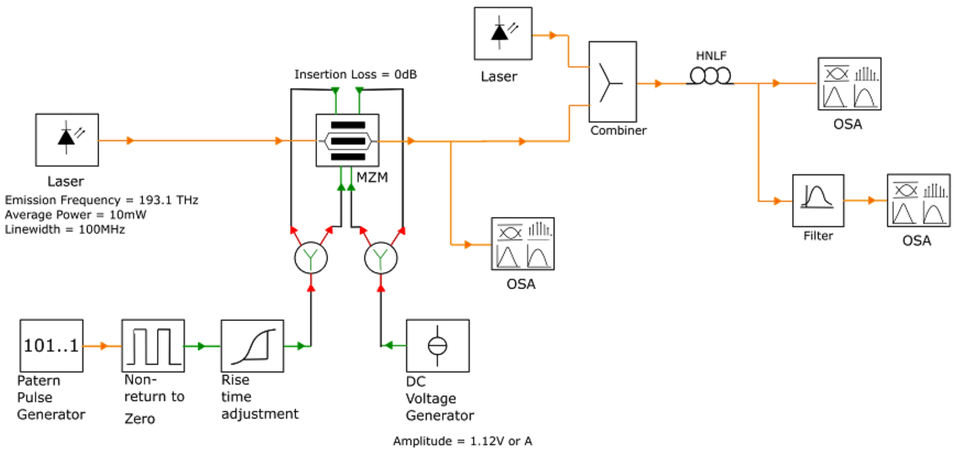

Figure 3.5: FWM schematic diagram with BPSK modulator

Previously modulated BPSK signal and a continuous wave laser pump signal (193.3 THz) was coupled, amplified and launched into a nonlinear media to participate in the degenerate FWM process. The nonlinear media is a HNLF with a zero-dispersion wavelength (ZDW) of 1554 nm, a nonlinear coefficient of 10 (W/km), a dispersion slope of 0.08 $ps/nm/km^2$, an effective area of 12 μm^2, and a fiber loss of 0.2 dB/km at 1550 nm [82]. The optical spectra after the FWM process were observed using an optical signal analyzer (OSA).

The output spectrum of the highly nonlinear fiber after the FWM process is shown in figure 3.6 (a). Since a BPSK signal is generated by multiplication of a sinusoidal high frequency carrier with a data signal of binary values, the resulting wave is spread over a range of wavelengths (frequencies). The Pump signal is a clean continuous wave laser output with a very narrow linewidth (single frequency). Output spectrum illustrates the newly generated idlers by confirming the FWM process. The recovered carrier at centered at 192.91 THz or idler 1 $(2fs - fp)$ was filtered using a 60 GHz Gaussian type filter [4].

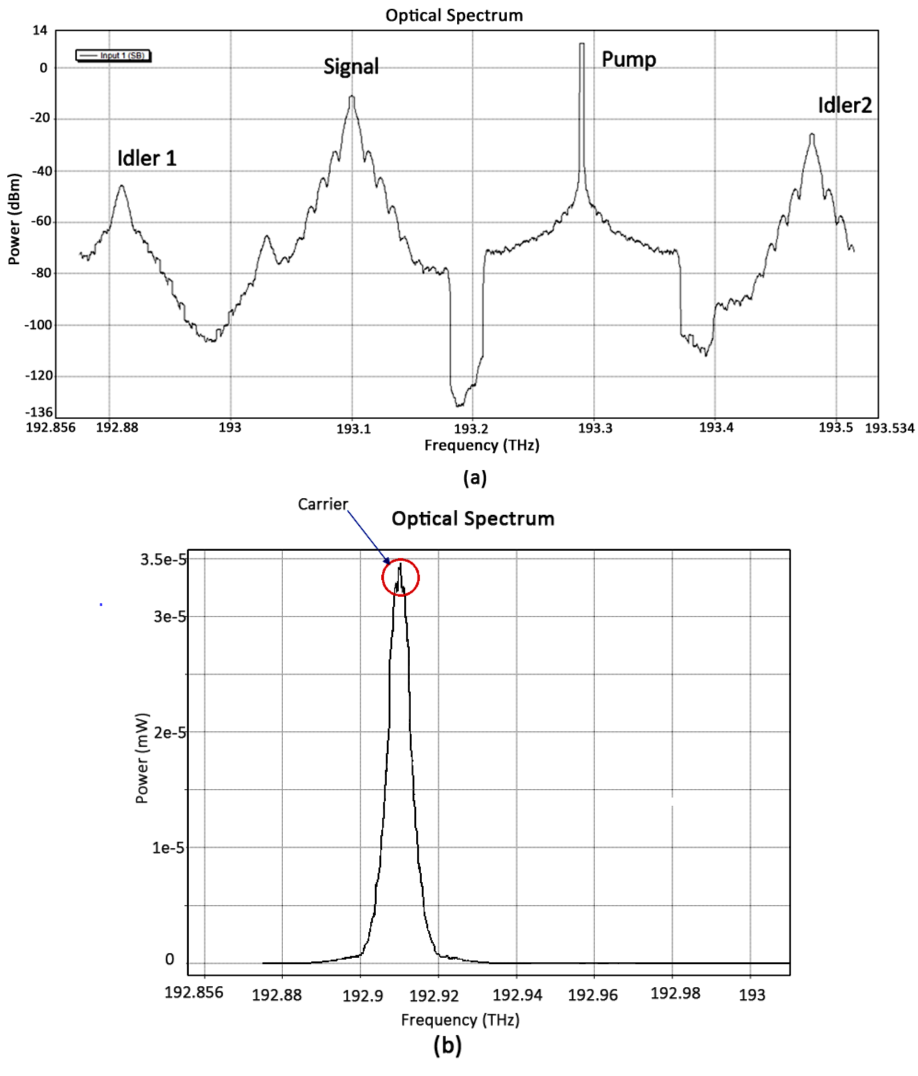

Figure 3.6: (a)-Four Wave Mixing Output, (b)- filtered idler 1 spectrum

Also, figure 3.6 (b) presents an enlarged image of idler 1 and it further confirmed that the modulation was stripped off from the incoming data signal and the phase information of the data laser was transferred to the idler 1.

Equation 2.9 defines the properties of the idler 1. According to the equation the field strength is squared and data gets filtered out. Since the data is filtered out, the idler only contains the remains of the data signal which is the carrier and pump signal. The amplitude and phase properties of the Idler 1 are identical to the carrier which proves that the carrier is recovered. The signal frequency is different from the frequency of the carrier. But using appropriate electronics, this recovered carrier can also be down-converted into the original carrier's frequency.

Chapter 4

SYSTEM CHARACTERIZATION FOR DEGRADING OSNR

4.1 Analysis

4.1.1 Theoretical

In this research, FWM is used as a phase modulation erasure technique from an incoming signal. Here, we use the degenerate FWM in a HNLF. The noise influences from the signal laser for the recovered carrier was investigated. For that, the linewidth of a recovered carrier was analyzed with various levels of OSNR and accumulated dispersion of an input modulated signal. Linewidth of a laser is often defined in terms of the FWHM of the optical field power spectrum [57]. The Delayed self-heterodyne method is known to be one of the most sensitive methods to analyze the laser linewidth. The FWHM linewidth of a laser is often measured with respect to the assumed Lorentzian spectral shape. The Lorentzian optical power spectrum ($S(f)$) centered at f_c has a functional form given by [57],

$$S(f) = \frac{1}{1 + (\frac{f-f_c}{\Delta v/2})^2} \tag{4.1}$$

where, f_c - Center frequency,
f -signal frequency,
Δv -Spectral linewidth,

The Linewidth broadening of the recovered optical carrier due to the OSNR and dispersion of an incoming signal is investigated theoretically and experimentally.

This experiment consists of 3 steps as shown in figure 4.1. These 3 steps were analyzed separately by directly connecting the laser signal as input and measuring the linewidth using delayed self-heterodyne linewidth measuring setup (figure 2.16).

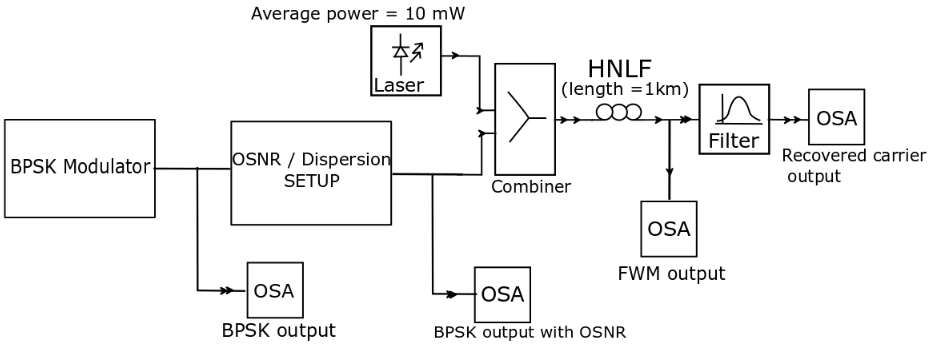

Figure 4.1: Schematic diagram for carrier extraction using FWM

4.1.1.1 Linewidth broadening due to the optical modulation

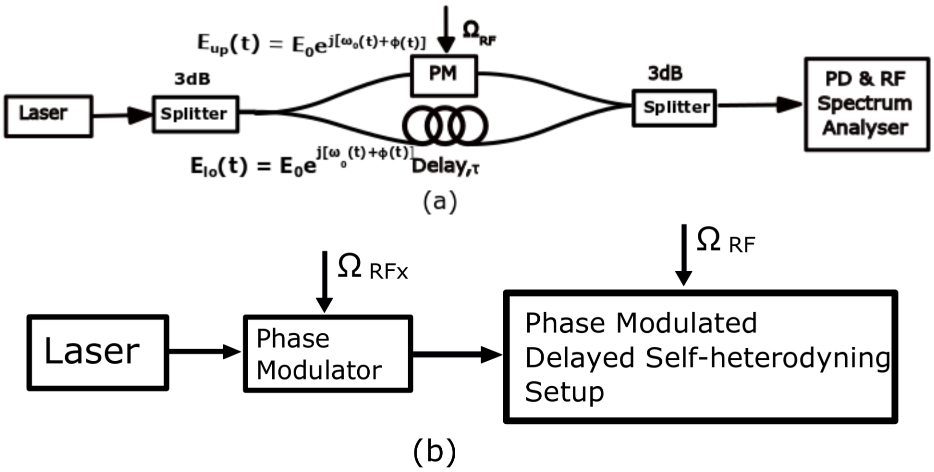

Figure 4.2: (a)-Phase modulated delayed self-heterodyning interferometric arrangement. [6] (b)- Linewidth measuring after modulation

The analysis of the modulation starts with analysing the phase modulated delayed self-heterodyne setup. The optical field equation of upper and lower arms of the interferometer (figure 4.2 (a)) is derived. At the photodetector, which is assumed to have unity responsivity, after τ delay time the output current produced is given as,

$$\begin{aligned} I(t,\tau) = 2E_0^2 &+ E_0^2 e^{j(\Phi(t)-\omega_0(\tau)-\Phi(t+\tau))} e^{jD\sin(\Omega_{R_F}t)} \\ &+ E_0^2 e^{-j(\Phi(t)-\omega_0(\tau)-\Phi(t+\tau))} e^{-jD\sin(-\Omega_{R_F}t)} \end{aligned} \tag{4.2}$$

Where,

E_0 - Optical field amplitude,
ω_0 - Optical frequency,
D - Modulating index,
Ω_{R_F} - Phase noise of the electrical signal,

$\phi(t)$ - Phase fluctuation function.

Using the Bessel function [6],

$$e^{jD\sin(\Omega_{R_F}(t))} = \Sigma_{m=-\infty}^{\infty} J_m(D) e^{jm\Omega_{R_F}(t)} \tag{4.3}$$

$$J_{-m}(D) = (-1)^m J_m(D) \tag{4.4}$$

where,

J - Bessel function,

m - order of the Bessel function,

rearranging the current produce by photo detector,

$$I(t,\tau) = 2E_0^2[1 + \Sigma_{m=-\infty}^{\infty} J_m(D)\cos\left(\Phi(t) - \omega_0(\tau) - \Phi(t+\tau) + m\Omega_{R_F}t\right] \tag{4.5}$$

Let,

$$\Phi(t) - \omega_0(\tau) - \Phi(t+\tau) = A \tag{4.6}$$

by substituting,

$$I(t,\tau) = 2E_0^2[1 + \Sigma_{m=-\infty}^{\infty} J_m(D)\cos\left(A + m\Omega_{R_F}t\right] \tag{4.7}$$

Spectral density of the signal is given by taking the Fourier transformation of the output current in equation 4.7 [116–118],

Therefore, spectral density of the laser is given by,

$$\begin{aligned} S(f_0) = {} & 2E_0^2[\sqrt{2\pi}\delta(f) \\ & + \Sigma_{m=-\infty}^{\infty} J_m(D)[\sqrt{\tfrac{\pi}{2}}(e^{-jA}\delta(f - m\Omega_{RF}) + e^{jA}\delta(f + m\Omega_{RF}))]] \end{aligned} \tag{4.8}$$

where, δ is the Dirac delta function.

Here the zeroth and first kind Bessel functions are considered. For m = 0, $J_0(D)$ = 1 and for m = 1, $J_1(D)$ = D/2.

By substituting on equation 4.8,

$$\begin{aligned} S(f_0) = {} & 2E_0^2[\sqrt{2\pi}\delta(f) + \sqrt{\frac{\pi}{2}}(e^{-jA}\delta(f) + e^{jA}\delta(f)) \\ & + \mathrm{D}/2\sqrt{\tfrac{\pi}{2}}(e^{-jA}\delta(f - \Omega_{RF}) + e^{jA}\delta(f + \Omega_{RF}))] \end{aligned} \tag{4.9}$$

If the input optical field to the delayed self-heterodyne is a phase modulated signal instead of an unmodulated laser (figure 4.2 (b)), the optical field after phase modulation can be written as,

$$E_{PM}(t) = E_0 e^{j(\omega_0(t)+\Phi(t)+D\sin(\Omega_{RFx}t))} \tag{4.10}$$

where, Ω_{RFx} is the phase noise of the phase modulator.

Output current of the photodetector (in the delayed self-heterodyne) corresponding to the phase modulated signal,

$$I(t,\tau) = 2E_0^2[1 + \Sigma_{m=-\infty}^{\infty} J_m(D)\cos(A + m\Omega_{R_F}t - m\Omega_{RFx}\tau)] \tag{4.11}$$

Spectral density of the signal is the Fourier transformation of the output current,

$$\begin{aligned} S(f) = 2E_0^2[\sqrt{2\pi}\delta(f) + \Sigma_{m=-\infty}^{\infty} J_m(D)[\sqrt{\pi/2}(e^{-j(A-m\Omega_{RFx}\tau)} \\ \delta(f - m\Omega_{RF}) + e^{j(A-m\Omega_{RFx}\tau)}\delta(f + m\Omega_{RF}))]] \end{aligned} \tag{4.12}$$

Similarly, let's consider only the zeroth and first kind of the Bessel functions. for m = 0, $J_0(D)$ = 1 and for m = 1, $J_1(D)$ = D/2.

by substituting to equation 4.12,

$$\begin{aligned} S(f) = 2E_0^2[\sqrt{2\pi}\delta(f) + \sqrt{\pi/2}(e^{-jA}\delta(f) + e^{jA}\delta(f)) \\ +\mathrm{D}/2\sqrt{\pi/2}(e^{-j(A-\Omega_{RFx}\tau)}\delta(f - \Omega_{RF}) + e^{j(A-\Omega_{RFx}\tau)}\delta(f + \Omega_{RF}))] \end{aligned} \tag{4.13}$$

From equation 4.9 and equation 4.13,

Spectral density of phase modulated signal,

$$\begin{aligned} S(f) = S(f_0) - D/2\sqrt{\pi/2}[e^{-jA}\delta(f - \Omega_{RF})(1 - e^{(j\Omega_{RFx}\tau)}) + e^{jA} \\ \delta(f + \Omega_{RF})(1 - e^{(-j\Omega_{RFx}\tau)})] \end{aligned} \tag{4.14}$$

According to the above equation, the signal strength shifts to the modified Lorentzian pedestal from the delta function peak with the increase of a delay time. This happens until the power spectrum becomes exactly Lorentzian [57, 119].

Therefore, using equation 4.1 the linewidth at FWHM of the phase modulated signal can be written as,

$$\Delta v = \frac{2(f - f_c)}{\sqrt{(1/S(f) - 1)}} \tag{4.15}$$

4.1.1.2 Linewidth broadening due to optical amplification

An EDFA is the most commonly used optical amplifier to compensate the loss of an optical fiber in long-distance optical communication. In an optical communication system with cascaded amplifiers, the spontaneous emission from optical amplifiers are accumulated and added to the transmitted signal. It deteriorates the optical signal to noise ratio (OSNR) of the signal [120]. The amplified spontaneous emission (ASE) noise is generated in the optical amplifier and it is considered as one of the main sources of noise that limits the performance of the phase modulated transmission system [121–124].

The ASE noise field can be expressed in terms of in-phase and quadrature-phase noise components as shown in figure 4.3.

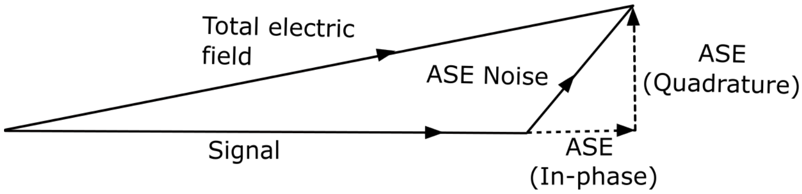

Figure 4.3: Vector representation of a signal and spontaneous emission.

The in-phase component becomes amplitude modulated (AM) noise of the signal and tyhe quadrature component serves as a phase modulated (PM) noise. Such PM noise directly increases the spectral linewidth of the signal and AM noise is converted into PM noise due to the Kerr nonlinearity of the optical fiber. It also gives rise to spectral linewidth broadening of the signal [125–127].

The linewidth broadening due to ASE arises from optical amplification is given by, [128, 129]

$$\Delta v = \frac{(n_{sp} h\nu B_0^2 (G-1))}{(a\pi G P_{in})} \tag{4.16}$$

where, n_{sp} - spontaneous emission factor,

h - planck's constant,

ν - frequency of signal,

G - gain of the amplifier,

B - bandwidth of the amplifier.

4.1.1.3 Linewidth broadening due to Four Wave Mixing

The degenerate FWM process generate two idlers [79–81] with phase(Φ_{ix}), frequency(ω_{ix}), and amplitude(E_{ix}) relationship as shown below [4, 34, 82]:

$$E_{i1} = E_s^2 \cdot E_p^* \cdot e^{(i((2\omega_s - \omega_p)t - (2\Phi_s - \Phi_p)))} \tag{4.17}$$

$$E_{i2} = E_p^2 \cdot E_s^* \cdot e^{(i((2\omega_p - \omega_s)t - (2\Phi_p - \Phi_s)))} \tag{4.18}$$

The frequency and phase of new idlers closer to the signal and pump can be written as:

$$\omega_{i1} = 2\omega_s - \omega_p \tag{4.19}$$

$$\omega_{i2} = 2\omega_p - \omega_s \tag{4.20}$$

$$\Phi_{i1} = 2\Phi_s - \Phi_p \tag{4.21}$$

$$\Phi_{i2} = 2\Phi_p - \Phi_s \tag{4.22}$$

Linewidth of the idler of our interest [130],

$$\Delta\nu_i = 2\Delta\nu_s - \Delta_p \tag{4.23}$$

where, the $\Delta\nu_s$ and Δ_p are signal and pump linewidth respectively.

4.1.2 Simulation

After successful carrier recovery, further experiments was carried out to confirm the OSNR tolerance of the system. The intended measurement were to degrade the input OSNR of the BPSK signal to the carrier recovery system.

To set the OSNR to the system, a variable optical attenuator and an EDFA placed after the BPSK transmitter. Then the total optical power was restored to a constant level using a second EDFA and a variable attenuator [131]. This signal was coupled with a continuous wave laser pump and launched into a HNLF to participate in the degenerate FWM process. The polarization controllers in front of the signal and the pump were used to achieve maximum efficiency for FWM process. The recovered idler was filtered out using a band-pass filter and the FWHM linewidth was measured using a delayed self-heterodyne technique [4,13].

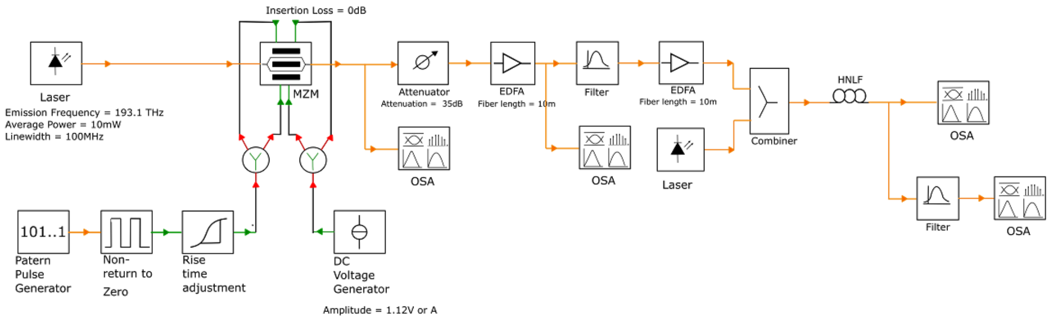

Figure 4.4: schematic diagram for carrier extraction under OSNR

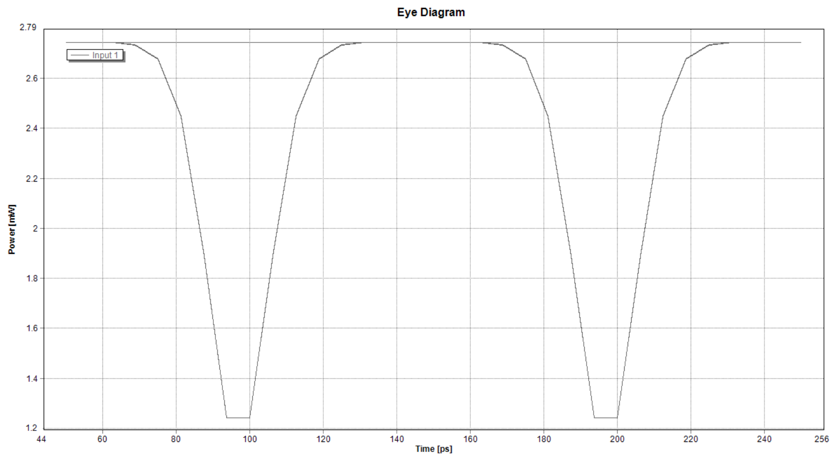

Figure 4.5: BPSK signal eye diagram before adding noise

Initially, the output of the HNLF Figure was observed using an OSA. Figure 5.4 shows the eye diagram variation of BPSK transmitted signal without any impairments. The visual information given by eye diagrams are very helpful to evaluate and troubleshoot the transmission systems. As shown in the figure, it is a clear eye diagram, it can be concluded this signal does not consist of amplitude or phase noise.

Figure 4.6 shows the captured eye diagram of the BPSK modulated signal for different levels of OSNR. According to figure 4.6, the amount of eye opening reduces with the degradation of the input OSNR value. The eye opening depicts the amplitude variation and OSNR degradation of the signal. Furthermore, the

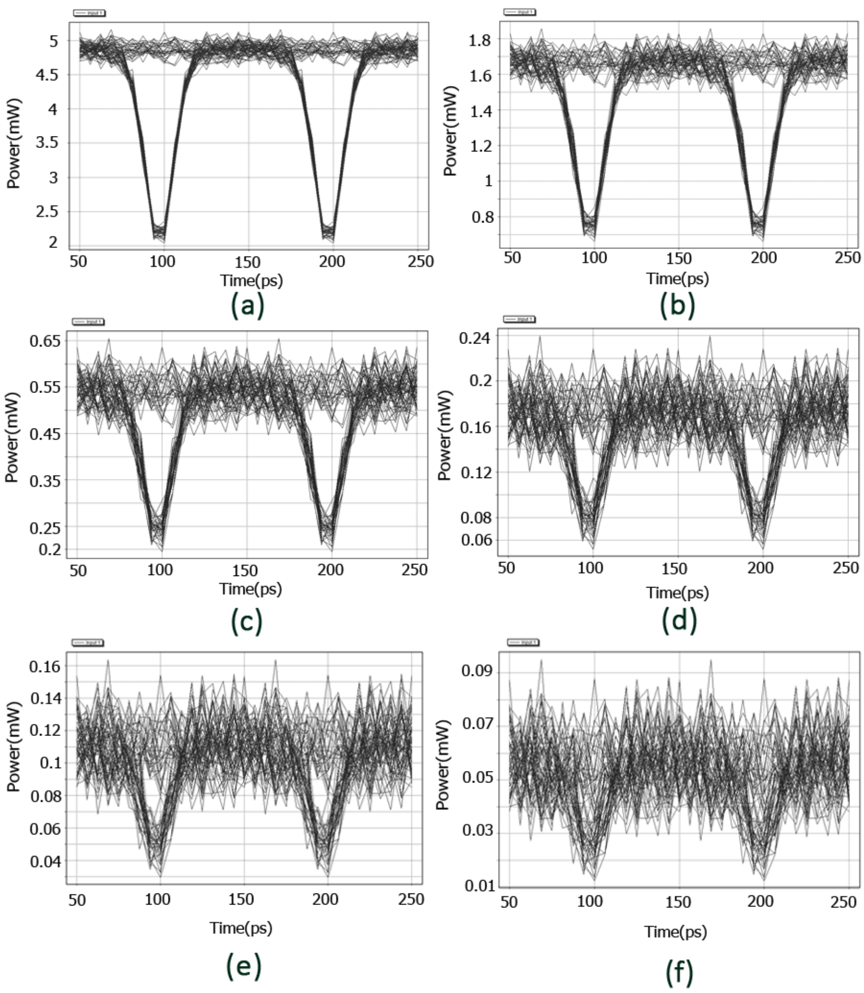

Figure 4.6: BPSK signal eye diagrams for different input OSNR values: (a) OSNR = 15.61 dB, (b) OSNR = 15.39 dB, (c) OSNR = 14.79 dB, (d) OSNR = 13.32 dB, (e) OSNR = 12.38 dB, (f) OSNR = 10.58 dB

data laser was re-tuned from the pump laser to have frequency separations Δf from 175 GHz to 200 GHz with 5 GHz steps during this analysis.

Figure 4.7 depicts the optical spectrum of recovered idler with the variation of input OSNR of BPSK signal. According to the figure, idler power (dBm) has been reduced with respect to the reduction of input OSNR value.

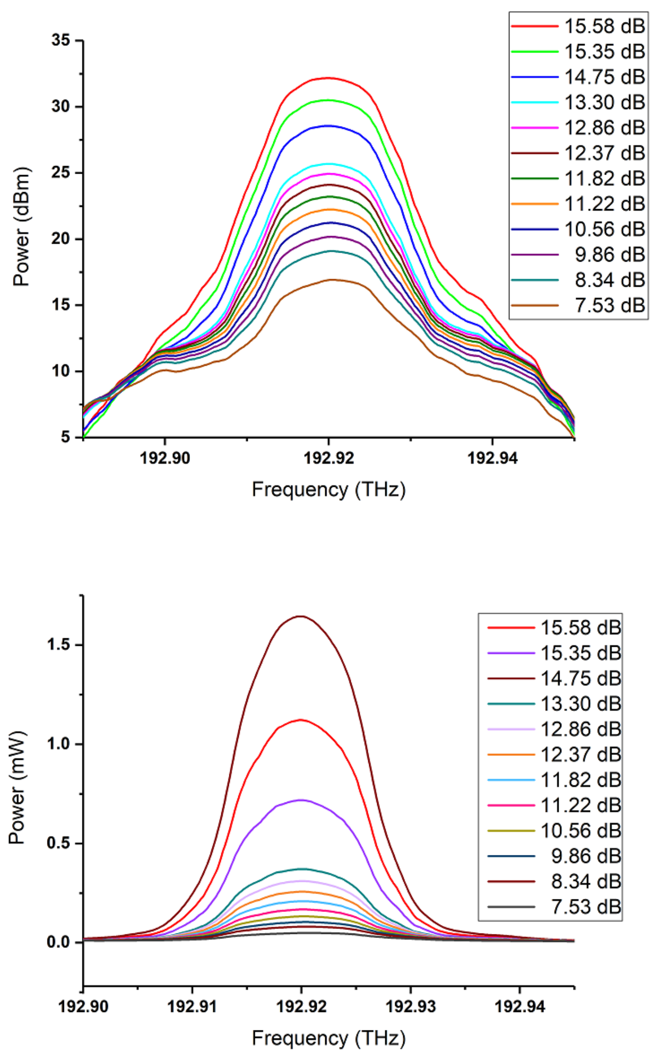

Figure 4.7: Power Variation of Idler with various input OSNR values (a)- Power in dBm, (b)- Power in mW

Figure 4.8 shows the linewidth variation of recovered carrier with various input OSNR values for (Δf =) 180 GHz, where Δf is the frequency separation between signal and pump. As shown in the figure, the extracted carrier had nearly constant linewidth measured for an input OSNR greater than 10 dBm. Since this figure represents the linewidth values in GHz range it might not be the exact value. Moreover, it is difficult to measure the linewidth for input OSNR less than 8 dBm.

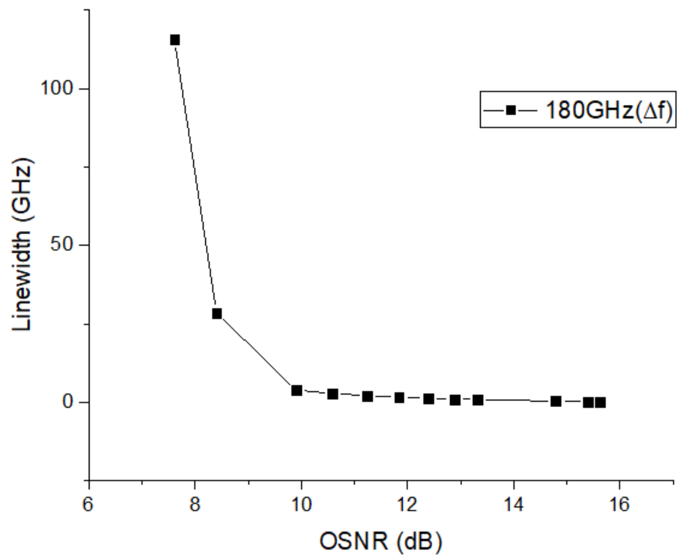

Figure 4.8: Linewidth Variation of Idler with various OSNR values for Δf 180GHz

The input OSNR of the BPSK signal of the carrier recovery setup was reduced and the effect of the linewidth for different Δf values were measured. The linewidths measured for the OSNR values up to 16 dBm were between 170-200 GHz at 10 GHz intervals for all the Δf variations is shown in figure 4.9. As shown in figure 4.9, the laser linewidth was increased dramatically for the input OSNR value of less than 10 dB. This figure represents the linewidth values in GHz range as well. The deviation visible in the frequency separation of 170 GHz between pump and signal separation is mainly due to the limitation of VPItransmissionMaker^{TM} software. The frequency separations (Δf) below 170 GHz was not able to simulate accurately in this software. With these limitations, the simulations were carried for a frequency separation (Δf) from 170 to 200 GHz, From figure 4.9 the behavior of recovered carrier linewidth can be observed and decided about the limiting parameters of the input OSNR values to operate the system accurately.

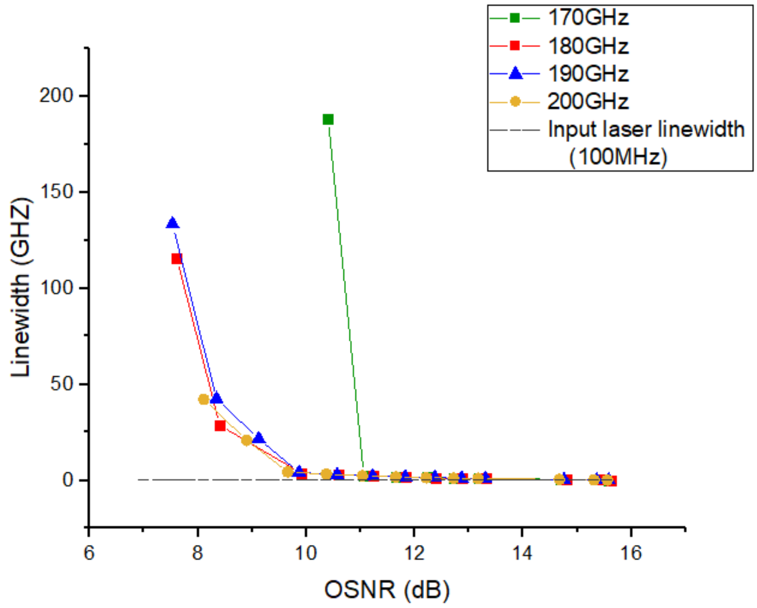

Figure 4.9: Measured linewidths vs Input OSNR for different Δf

The influence of the linewidth of the recovered carrier against different OSNR was investigated for a frequency separation of (Δf =) 190 GHz where Δf is the frequency separation between signal and pump. The extracted carried had a linewidth of 149.11 MHz. As shown in figure 4.10, the extracted carrier had a nearly constant linewidth (LW = 149.11 MHz) for an input OSNR greater than 14.32 dB.

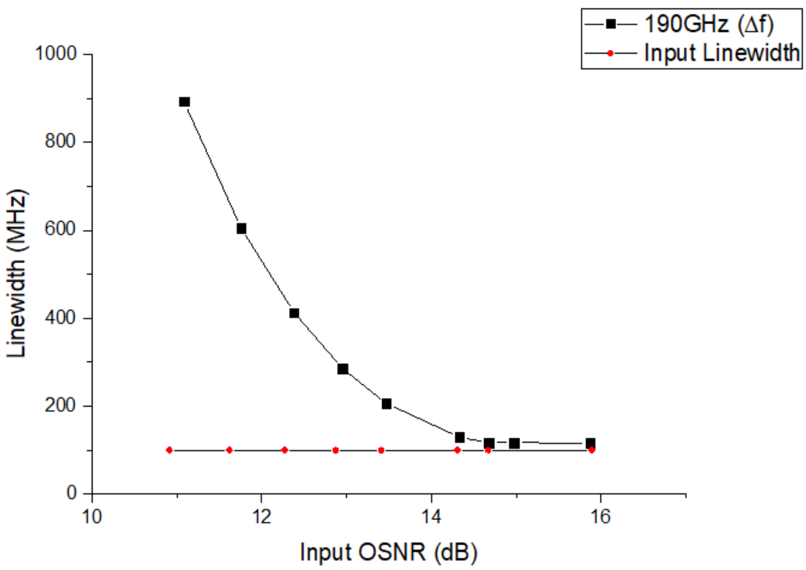

Figure 4.10: Linewidth variation of idler with various OSNR values for Δf of 190 GHz

The input OSNR of the BPSK signal of the carrier recovery setup was reduced and the effect of the linewidth for different Δf values was measured. The linewidths measured for the OSNR values up to 16 dBm was between 175-200 GHz at 5 GHz intervals for all the Δf variations. The laser linewidth was increased dramatically for the input OSNR value of less than 14.32 dB (figure 4.11). According to equation 4.17, recovered carrier power and the signal power has a quadratic relationship, and the reduction in signal power through the degradation of OSNR, is the reason for the reduction of idler power. Decreasing of idler power causes the increase in idler linewidth.

It is obvious that the same carrier information with a slightly broadened linewidth can be obtained. The system can tolerate a constant recovered linewidth up to 14.32 dB. Hence, by combining this scheme with injection locking a more cleaned narrower linewidth can be generated [13]. This narrow linewidth laser is more suitable for achieving phase synchronization in higher performance in the PSA, optical synchronization schemes and Optical homodyne receivers.

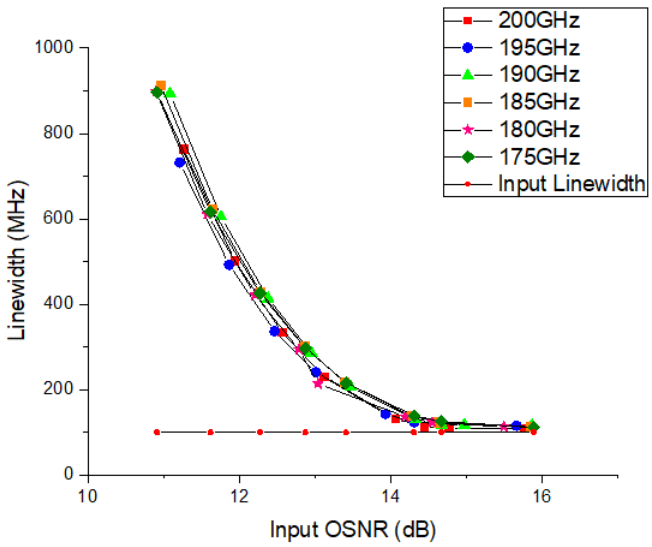

Figure 4.11: Measured linewidths vs Input OSNR for different Δf

Linewidth broadening of a phase modulated signal was calculated using equations 4.9, 4.14 and 4.15 and linewidth broadening of an amplified signal was calculated using equation 4.16. For an initial input signal with 100 MHz linewidth, the percentage of theoretically calculated linewidth broadening and the percentage of simulated linewidth broadening is tabulated in Table 4.1.

Table 4.1: Linewidth broadening value

	Calculated Value	**Measured Value**
After phase modulation	13.92 %	14.67%
After amplification	0.036 %	0.101 %

The FWM idler linewidth for BPSK modulated and pre-amplified signal is calculated using equation 4.23. According to the calculation, the idler linewidth broadening value is 27.92 MHz and the measured linewidth broadening value is 34.34 MHz. Therefore, it can be concluded that the measured linewidth broadening values are in good agreement with the theoretically calculated linewidth broadening values. The calculated value of the idler linewidth which underwent the phase modulation, amplification and the FWM process is, 127.92 MHz and the measured value is, 134.34 MHz.

Chapter 5

CHARACTERIZATION FOR ACCUMULATED DISPERSION

The accumulated dispersion analysis was carried out for the carrier recovery system to inspect the dispersion tolerance of the system. The chromatic dispersion mainly depends on the dispersion parameter of the fiber, the spectral width of the data pulse, the center wavelength of the data pulse and the uncompensated length of the fiber which the data traverse. In this simulation, the length of the fiber was changed to introduce a controlled amount of chromatic dispersion to the system.

To set the dispersion, the OSNR setup (figure 4.1) was replaced with the different lengths of single mode fiber (SMF) [4]. As shown in figure 5.1 It was placed after the BPSK transmitter to vary the dispersion at the input of the FWM setup. The dispersed data signal was coupled with a continuous wave laser pump signal and launched into a HNLF to participate in the degenerate FWM process. Similar to the OSNR setup, the recovered idler was filtered using a band-pass filter and the FWHM linewidth was measured.

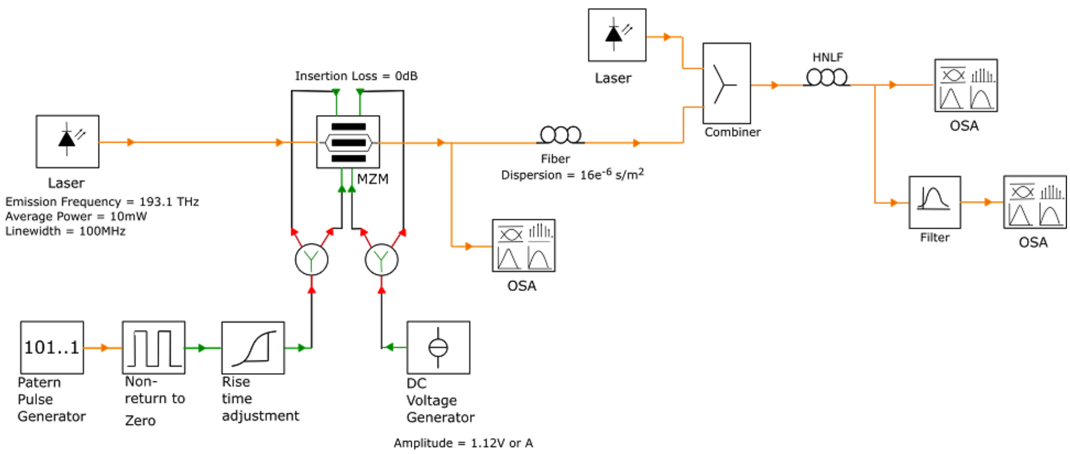

Figure 5.1: schematic diagram for carrier extraction under OSNR

The captured eye diagram of the input BPSK modulated signal is represent in figure 5.2 for different level of dispersion.

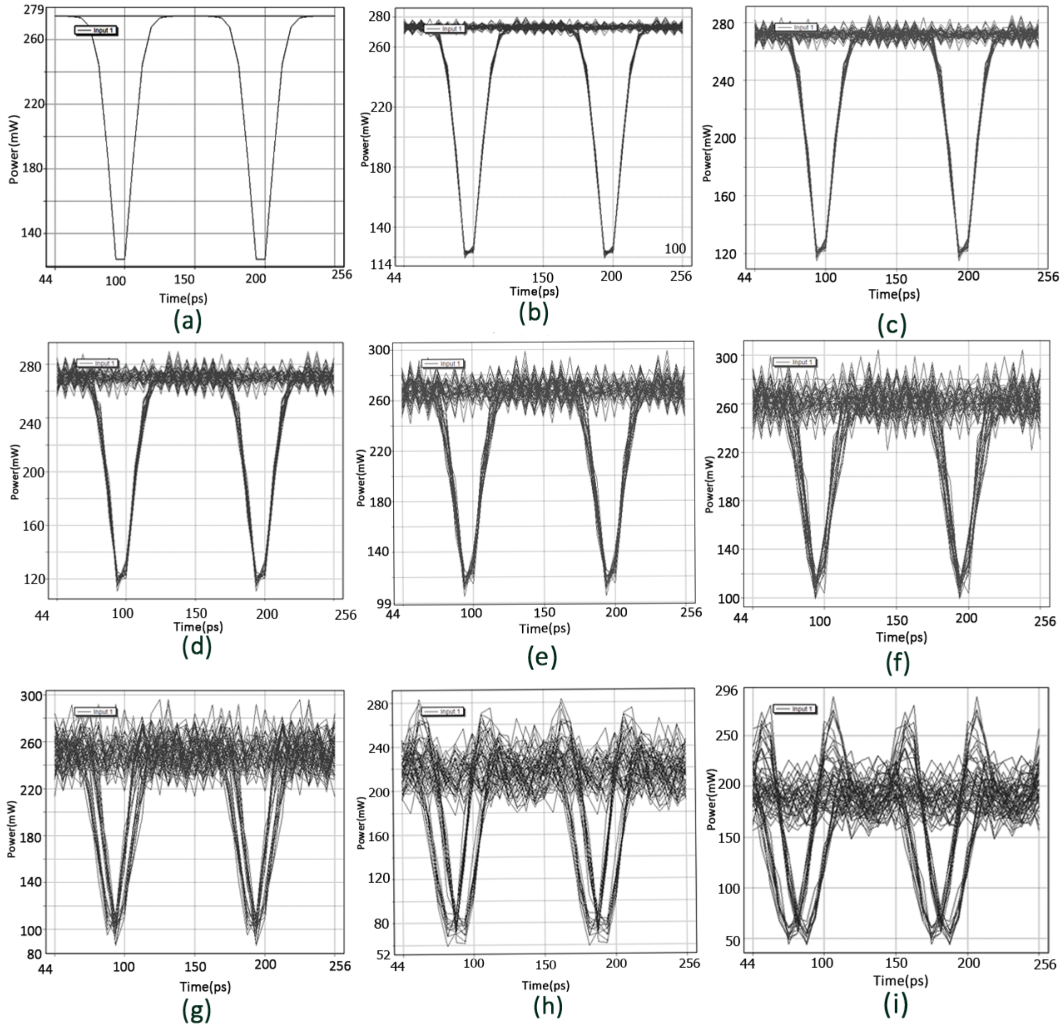

Figure 5.2: BPSK signal eye diagrams for different input Dispersion values: (a) 0 ps/nm, (b) 1.6 ps/nm, (c) 3.2 ps/nm, (d) 4.8 ps/nm, (e) 8 ps/nm, (f) 16 ps/nm, (g) 32 ps/nm, (h) 80 ps/nm, (i) 128 ps/nm

According to the eye diagram, it can be seen that the noise in both amplitude and time has been increasing with increased dispersion. Eye opening value is nearly equals to 152 mW at the zero dispersion tolerance.

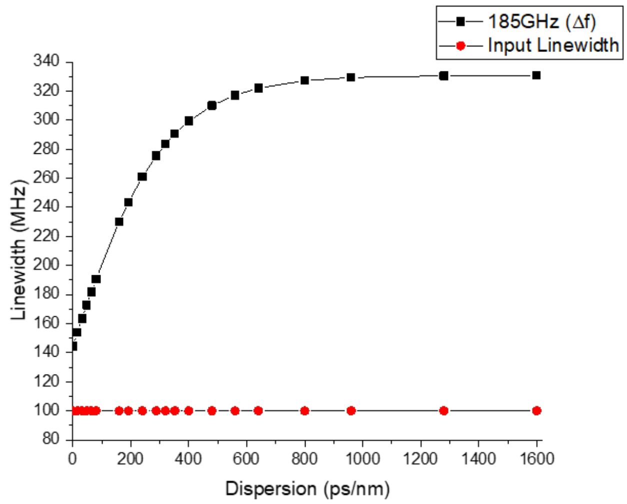

Figure 5.3: Linewidth variation of idler with various dispersion values for Δf of 185 GHz

Figure 5.3 depicts the linewidth variation of the recovered carrier with various dispersion values for Δf of 185 GHz. As shown in the figure, the measured linewidth began to saturate after a higher dispersion value (greater than 70 ps/nm). The reason for this might be, even though the eye opening is fairly good (fairly better OSNR) an increased timing jitter will affect the carrier recovery and the system might collapse.

During the simulation, the OSNR value is kept at a fixed level at 14.78 dB and it has a very low ASE noise. Here the system tolerance for the dispersion was evaluated. Due to the limitations in the simulation software, it is difficult to observe a clear idler spectrum (or recovered carrier) for higher dispersion values after 100 ps/nm. As a result of that, the linewidth values converged to the same level. Therefore, to display more accurate results by eliminating the limitations due to the simulator, the independent axis values were limited up to 80 ps/nm.

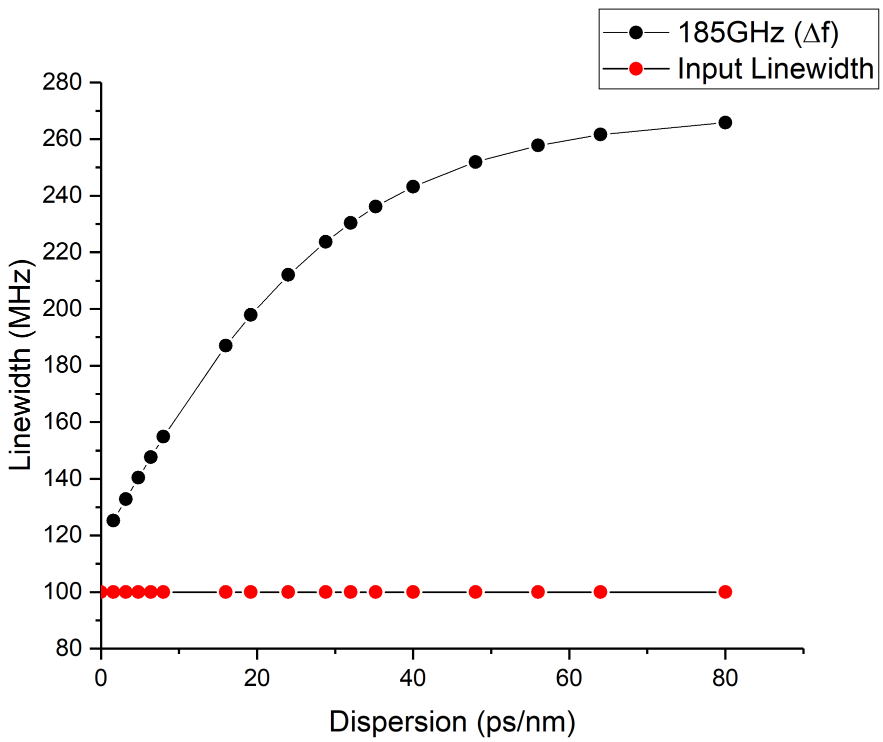

Figure 5.4: Linewidth variation of idler with various dispersion values for Δf of 185 GHz

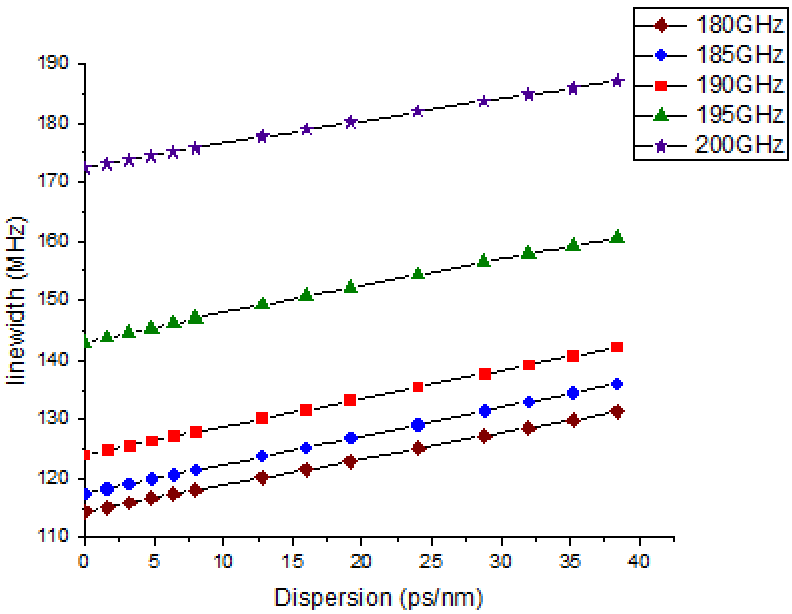

Figure 5.5: Measured linewidths against the accumulated dispersion for different Δf

The linewidth measurement for the dispersion value up to 38.4 ps/nm is shown in figure 5.5. The frequency separation between the pump and the data signal was changed between 180-200 GHz at 5 GHz intervals for all the Δf variations. It is noted that with increased Δf values the recovered linewidth is increased. The linewidth increment for zero dispersion value for different signal pump separation is mainly due to the reduction in the FWM conversion efficiency. This FWM efficiency reduction has an impact on the modulation stripping system with the increment of the frequency separation between pump and signal.

Chapter 6

CONCLUSION AND FUTURE WORK

The research presented in this thesis is all about the behavior of the FWM based carrier recovery system for OSNR and dispersion degradation. Under the optical carrier recovery, FWM based carrier recovery system was simulated using VPItransmissionMaker^{TM} optical systems software and HNLF was used to perform FWM by reducing other non linear effects. The impairment effects present in the practical system was simulated for BPSK modulated signals. In conclusion, the theoretical concept of FWM was proved by the results generated by simulation.

The recovered linewidth value was broadened by 27.92 MHz in the theoretical examination conducted for checking the effect of input OSNR of the BPSK modulated signal on the linewidth of the recovered carrier. This theoretical examination was evaluated separately by dividing the whole system into three sections and the recovered carrier linewidth was measured using the delayed self heterodyne method. Both modulation and FWM make considerable contributions towards the linewidth variation. However, ASE noise generated through amplification does make a low contribution to the linewidth broadening.

The experimental assessment has started with simulating the effect of input OSNR of BPSK modulated signal on the linewidth of the recovered carrier. The results denote that the recovered carrier linewidth is increasing with more additive noise power. The recovered linewidth was dramatically decreasing with the increase of the input OSNR values. The recovered carrier had a nearly constant linewidth value from input OSNR value became 14.32 dB. Therefore, the system is working properly for an OSNR value greater than 14.32 dB for different pump and signal separations. Both theoretical and experimental analysis brought up the conclusion that the theoretical and measured linewidth broadening values are in good agreement with each other.

Furthermore, we have analyzed the linewidth of the recovered carrier for different dispersion values of the input BPSK modulated signal and observed that linewidth is increasing with the dispersion value. Also, at the higher dispersion value the measured linewidth was started to saturate due to the timing jitter effect on the carrier recovery. Therefore, a proper dispersion compensation (up to 80 ps/nm) should be employed for better performance.

6.1 Future developments

This research was only carried out in implementation carrier recovery and characterization for OSNR and dispersion. But this achievement of carrier recovery can be used in applications in ultra-high speed optical communications and coherent optical receivers to process homodyne receiving, signal regeneration, synchronization, format conversion, etc

The carrier recovery method is based on only one nonlinear phenomenon which is FWM. Therefore, in this research it was considered only the FWM effect by reducing other nonlinear effects. In reality, there are many more nonlinear effects degrading the quality of carrier recovery such as self and cross phase modulations, scattering, back propagation and harmonic generations. The research can be expanded using these effects and their impact on carrier recovery.

This carrier recovery and characterizing were demonstrated using BPSK modulated signal. But this carrier recovery technology and characterization can be extended to DPSK, QPSK schemes and other MPSK schemes.

References

[1] "Dispersion compensating fiber," https://www.thorlabs.com/catalogpages/obsolete/2017/DCF38.pdf, accessed: 2020-10-10.

[2] "What is zero water peak fiber?" https://www.fiberoptics4sale.com/blogs/archive-posts/95050054-what-is-zero-water-peak-fiber, accessed: 2020-10-10.

[3] X. Chen, "Ultra-narrow laser linewidth measurement." Virginia Polytechnic Institute and State University, 2006, pp. 17–27.

[4] R. U. Weerasuriya, "Data retiming for multi-wavelength regeneration," Ph.D. dissertation, Ireland, 2011.

[5] J. J. Hamd-Ameen, "Dispersion and intersymbol interference (isi) in optical fibers," *International Conference on Communication, Computer Power (ICCCP'07)*, p. 366, February 2007.

[6] L. V. T. Nguyen, in *Distributed feedback (DFB) laser coherence and linewidth broadening.* Defence Science and Technology Organization, 2003, pp. 1–44.

[7] P.Frascella, "Dpsk signal regeneration with a dual-pump non-degenerate phase-sensitive amplifier," *Photonic Technology Letters*, vol. 23, no. 8, pp. 516–518, 2011.

[8] J. M. Senior, "Optical fiber communications," in *Proceedings of the 23rd Annual Conference on Computer Graphics and Interactive Techniques.* UK:Pearson Education Limited, 2009.

[9] R.Slavık, "All-optical phase and amplitude regenerator for next-generation telecommunications systems," *Nature Photonic*, vol. 4, no. 2, pp. 690–695, 2010.

[10] R.Weerasuriya and et al, "Novel carrier extraction scheme for phase modulated signals using feed-forward based modulation stripping," *Optical Society of America*, pp. 19–23, 2010.

[11] C. Cheng and et al, "Measurement of the carrier recovery time in soa based on dual pump fwm," in n asia communications and photonics conference and exhibition," *Asia Communications and Photonics conference and Exhibition (ACP), Optical Society of America*, 2009.

[12] K.-T. Wu and H. Sun, "Techniques in carrier recovery for optical coherent systems," in *OFC/NFOEC*. Technical Digest of Optical Society of America, 2012, p. paper OTh4c.3.

[13] R.Weerasuriya and et al, "Generation of frequency symmetric signal from a bpsk input for phase sensitive amplification," *Optical Society of America*, 2010.

[14] T. Maiman, "Stimulated optical radiation in ruby," *Nature*, vol. 187, pp. 493–494, 1960.

[15] F. P. Kapron and et al, "Radiation losses in glass optical waveguides," *Applied Physics Letters*, vol. 17, pp. 423–425, 1970.

[16] G. Agrawal, "Fiber optics communication system," 2002, pp. 1–18.

[17] S. Tomaru and et al, "Vad single mode fibre with 0 2 db/km loss," *ELECTRONICS LETTERS*, vol. 17, no. 02, pp. 92–93, 1981.

[18] H. Kanamori and et al, "Transmission characteristics and reliability of pure-silica-core single- mode-fibers," *Journal of Lightwave technology*, vol. 04, pp. 1144–1150, 1986.

[19] K. Nagayama and et al, "Ultra low loss (0.151 db/km) fiber and its impact on submarine transmission systems," *Optical Fiber communication conference and exhibits*, pp. FA10–1– FA10–3, 2002.

[20] T. Miya and et al, "Ultimate low-loss single-mode fibre at 1.55 μm," *Electronic Letters*, vol. 15, no. 4, pp. 106–108, 1979.

[21] R. Linke and A. Gnauck, "High-capacity coherent lightwave system," *Journal of Lightwave technology*, vol. 06, no. 11, pp. 1750–1769, 1988.

[22] P. Henry, "Lightwave primer," *IEEE Journal of Quantum Electronics*, vol. 21, no. 12, pp. 1862–1879, 1985.

[23] N. S. Bergano and et al, "A 9000 km 5 gb/s and 21,000 km 2.4 gb/s feasibility demonstration of transoceanic edfa systems using a circulating loop," *Fiber Optic Communication*, vol. 4, p. PD 13, 1991.

[24] K. Fukuchi and et al, "10.92-tb/s (273 x 40-gb/s) triple-band/ultra-dense wdm optical-repeatered transmission experiment," *Optical Fiber Communication Conference and International Conference on Quantum Information*, p. PD 24, 2001.

[25] G. Vareille and et al, "3 tbit/s (300 x 11.6 gbit/s) transmission over 7380 km using c+l band with 25 ghz channel spacing and nrz format," *Optical Fiber Communication Conference and International Conference on Quantum Information*, p. PD 22, 2001.

[26] K. Schuh and et al, "1 t bit/s (10 x 107 gbit/s etdm) serial nrz transmission over 480km ssmf," *Optical Fiber Communication Conference and Exposition and The National Fiber Optic Engineers Conference*, p. PDP23, 2007.

[27] G. A. Thomas and et al, "Towards the clarity limit in optical fiber," *Nature*, vol. 404, pp. 262–264, 2000.

[28] W. J. Smith, "Modern optical engineering (3rd edn)." McGraw Hill, 2000.

[29] R. L. Freeman, "Fundamentals of telecommunication." John Wiley and Sons, 1999.

[30] F. L. Pedrotti and et al, "introduction to optics (3rd edn)." Prentice Hall, 2006.

[31] E. Hecht and A. Zajac, "Optics (4th edn)." Addison-Wesley, 2003.

[32] F. Graham and et al, "Optics and photonics: An introduction (2nd edn)." John Wiley and sons publication, 2007.

[33] G. P. Agrawal, "Lightwave technology." John Wiley and sons publication, 2005.

[34] G. Agrawal, "Nonlinear fiber optics," 2007.

[35] R. Ramaswami and K. Sivarajan, "A practical perspective," in *Optical Networks*, 2002, pp. 43–54.

[36] K. P. ho, "Phase modulated optical communication systems." Springer, 2005, pp. 1–40, 118–128, 129–137.

[37] S. Jawla, "Intensity modulation formats in optical communication system," *International Journal of Scientific & Engineering Research*, vol. 4, no. 4, 2013.

[38] E. IP and J. M. Kahn, "Power spectra of return-to-zero optical signals," *Journal of Lightwave Technology*, vol. 24, pp. 1610–1618, 2006.

[39] P. J. Winzer and R. J. Essiamber, "Advance modulation format for high capacity optical transport network," *Journal of Lightwave Technology*, vol. 24, pp. 4711–4728, 2006.

[40] R. Singh and S. Jawla, "Different modulation formats used in optical communication," *IOSR Journal of Electronics and Communication Engineering (IOSR-JECE)*, vol. 8, no. 4, 2013.

[41] "Frequency shift keying," https://www.tutorialspoint.com/digital_communication/digital_communication_frequency_shift_keying.htm, accessed: 2020-10-06.

[42] G. Breed, "A tutorial introduction to optical modulation techniques," *High Frequency design optical Modulation, Summit Technical Media*, 2007.

[43] A. H. Gnauck and P. J. Winzer, "Optical phase-shift-keyed transmission," *Journal of Lightwave Technology*, vol. 23, no. 1, pp. 115–130, 2005.

[44] T. Chikama and et al, "Modulation and demodulation techniques in optical heterodyne psk transmission systems," *Journal of Lightwave Technology*, vol. 8, no. 3, pp. 309–322, 1990.

[45] "Understanding quadrature phase shift keying (qpsk) modulation," https://www.allaboutcircuits.com/technical-articles/quadrature-phase-shift-keying-qpsk-modulation/, accessed: 2020-10-28.

[46] C. H. Henry, "Theory of the linewidth of semiconductor laser," *IEEE Journal of Quantum Electronics*, vol. QE-18, no. 02, pp. 259–264, 1982.

[47] M. Fleming and A. Mooradian, "Fundamental line broadening of single-mode (gaal)as diode lasers," *Applied Physics Letters*, vol. 38, pp. 511–513, 1981.

[48] M. Lax, "Classical noise. v. noise in self-sustained oscillators," *Physical Review Journals Archive*, vol. 160, pp. 290–307, Aug 1967.

[49] K. Vahala and A. Yariv, "Semiclassical theory of noise in semiconductor lasers-part i," *IEEE JOURNAL OF QUANTUM ELECTRONICS*, vol. 19, pp. 1096–1101, June 1983.

[50] M. Lax, "Quantum noise x density-matrix treatment of field and population-difference fluctuations," *Physical Review Journals Archive*, vol. 157, pp. 213–231, May 1967.

[51] J. van der Ziel, "Spectral broadening of pulsating alxga1-xas double heterostructure lasers," *IEEE Journal of Quantum Electronics*, vol. 15, no. 11, pp. 1277–1281, 1979.

[52] B. W. Hakki, "Optical and microwave instabilities in injection lasers," *Journal of Applied Physics*, vol. 51, no. 1, pp. 68–73, 1980.

[53] "My laser spectrum," http://mylaserspectrum.com/2018/02/spectral-purity-laser-assessed/, accessed: 2020-11-10.

[54] n. y. Voo and et al, "Linewidth and phase noise characteristics of dfb fibre lasers," *Proceedings of SPIE - The International Society for Optical Engineering*, vol. 5620, 12 2004.

[55] "Laser spectral linewidth," *NKT Photonics*, no. 09, 2013.

[56] "Full width half maximum," https://www.schoolsobservatory.org/discover/projects/clusters/fwhm, accessed: 2020-11-10.

[57] D. Derickson, in *Fiber Optic Test and Measurement.* Prentice Hall PTR, 1998, pp. 169–191, 475–486.

[58] R. Tkach and A. Chraplyvy, "Phase noise and linewidth in an ingaasp dfb laser," *Journal of Lightwave Technology*, vol. 4, no. 11, pp. 1711–1716, 1986.

[59] H. Qi, W. Wang, G. Guo, and Z. Song, "A practical perspective," in *Handbook of Optical Fibers.* springer, Singapore, 2018.

[60] "Ultra-narrow laser linewidth measurement," https://vtechworks.lib.vt.edu/handle/10919/11124, accessed: 2020-10-04.

[61] O. Ishida, "Delayed-self-heterodyne measurement of laser frequency fluctuations," *Journal of Lightwave Technology*, vol. 9, no. 11, pp. 1528–1533, 1991.

[62] L. B. Mercer, "1/f frequency noise effects on self-heterodyne linewidth measurements," *Journal of Lightwave Technology*, vol. 9, no. 4, pp. 485–493, 1991.

[63] I. Blekhman, "Synchronization in science and technology." ASME Press, 1988.

[64] M. G. Rosenblum, "Phase synchronization of chaotic oscillators," *American Physical society*, vol. 76, no. 11, pp. 1804–1807, 1996.

[65] V. Ferrero and S. Camatel, "Optical phase locking techniques: an overview and a novel method based on single side sub-carrier modulation," *Opt. Express*, vol. 16, no. 2, pp. 818–828, Jan 2008.

[66] T. Xu and et al, "A carrier synchronization method for global synchronous pulse width modulation application using phase-locked-loop," *IEEE Transactions on Power Electronics*, 02 2019.

[67] https://www.slideshare.net/FuyunLing/phaselocked-loop-pll-and-carrier-synchronization-fuyun lingv13.

[68] K. Iwashita and K. Nakagawa, "Suppression of mode partition noise by laser diode light injection," *IEEE Journal of Quantum Electronics*, vol. 18, no. 10, pp. 1669–1674, 1982.

[69] K. K. A. Murakami and K. Atsuki, "Cavity resonance shift and bandwidth enhancement in semiconductor lasers with strong light injection," *IEEE Journal of Quantum Electronics*, vol. 39, no. 10, pp. 1196–1204, 2003.

[70] C. H. Henry, "Locking range and stability of injection locked 1.54 pm ingaasp semiconductor lasers," *IEEE Journal Of Quantum Electronics*, vol. 21, no. 08, pp. 1152–1157, August 1985.

[71] L. Winkelmann and et al, "Injection-locked single-frequency laser with an output power," *Applied Physics*, vol. 102, pp. 529–538, February 2011.

[72] N. Schunk and K. Petermann, "Noise analysis of injection-locked semiconductor injection lasers," *IEEE Journal of Quantum Electronics*, vol. 22, no. 5, pp. 642–650, 1986.

[73] W. Han and et al, "The optical injection locking technique and its applications for wdm-pon spare function," *Proceedings of SPIE - The International Society for Optical Engineering*, vol. 7278, 2009.

[74] R. W. Boyd, "Nonlinear optics." Elsevier Publications, 2011, p. Chapter 1.

[75] E. Ip and J. M. Kahn, "Feedforward carrier recovery for coherent optical communications," *Journal of Lightwave Technology*, vol. 25, no. 9, pp. 2675–2692, 2007.

[76] R. Ramaswami and G. H. Sivaragan, "Optical networks (3rd edn)." Elsevier Publications, 2010, pp. 78–95, 314–325.

[77] M. Hofer and et al, "Mode locking with cross-phase and self-phase modulation," *Opt. Lett.*, vol. 16, no. 7, pp. 502–504, Apr 1991.

[78] A. Hasegawa and F. Tappert, "Transmission of stationary nonlinear optical pulses in dispersive dielectric fibers. i. anomalous dispersion," *Applied Physics Letters*, vol. 23, no. 3, pp. 142–144, 1973.

[79] K. Inoue, "Four-wave mixing in an optical fiber in the zero-dispersion wavelength region," *Journl of Lightwave Technology*, vol. 10, no. 11, pp. 1553–1563, 1992.

[80] N. Shibata, "Phase-mismatch dependence of efficiency of wave generation through four-wave mixing in a singal mode optical fiber," *IEEE journal of quntum electronics*, vol. 23, no. 07, pp. 1205–1211, 1987.

[81] K.Inoue, "Wavelength conversion experiment using fiber four-wave mixing," *IEEE Photonic Technology letters*, vol. 4, no. 01, pp. 69–73, 1992.

[82] M. T. Osamu Aso and S. Namiki, "Four-wave mixing in optical fibers and its applications," *Furukawa Review*, no. 19, pp. 63–68, 2000.

[83] X. Yang and et al, "Four-wave-mixing-assisted room-temperature four-wavelength erbium-doped fiber lasers," *Optical Engineering - OPT ENG*, vol. 45, 06 2006.

[84] S. Tomaru and et al, “Vad single mode fibre with 0 2 db/km loss,” *Electronics Lwtters*, vol. 17, no. 2, pp. 92–93, 1981.

[85] K. Nagayama and et a, “ultra low loss (0.151 db/km) fiber and its impact onsubmarine transmission systems,” *Optical Fiber communication conference and exhibits*, pp. FA10–1–FA10–3, 2002.

[86] A. C. Cokrak and A. Altuncu, “Gain and noise figure performance of erbium doped fiber amplifiers (edfa),” *Journal of Electrical and Electronics Engineering*, vol. 04, no. 2, pp. 1111–1122, 2004.

[87] S. M. J. Alam and et al, “Bit error rate optimization in fiber optic communications,” *International Journal of Machine Learning and Computing*, vol. 01, no. 5, pp. 435–440, 2011.

[88] R. Application note, HFAN-9.0.2, “Optical signal-to-noise ratio and the q-factor in fiber-optic communication systems.” Maxim integrated, 04/08.

[89] K. Lau, “Signal to noise ratio calculation for fiber optic links.” TDA Progress Report, Communication Systems Research Section, Jet Propulsion Laboratory, 1980, pp. 41–48.

[90] “Dispersion,” https://www.daenotes.com/electronics/communication-system/dispersion, accessed: 2020-11-03.

[91] P. J. Winzer and R. J. Essiambre, “Advanced optical modulation formats,” *Proceedings of the IEEE*, vol. 94, no. 5, pp. 952–985, 2006.

[92] J. c. Daly and I. D. Aggrawal, “Optical waveguide manufacturing,” in *Fiber Optics*, 1984, pp. 22–40.

[93] “Optical fiber dispersion,” https://www.fiberoptics4sale.com/blogs/archive-posts/95047942-optical-fiber-dispersion, accessed: 2020-11-03.

[94] R.Weerasuriya and et al, “Chromatic dispersion tolerance of 42.65gbit/s dual gate asynchronous digital optical regenerator,” *Photonics Ireland*, 2009.

[95] P. Pecci and et al, “Tolerance to dispersion compensation parameters of six,” *Electronics Letters*, vol. 39, no. 25, pp. 1844–1846, 2003.

[96] B. Clesca and et al, "The wdm answer to line-rate increase within the terrestrial fiber-based networks," in *Proceedings of GLOBECOM'96. 1996 IEEE Global Telecommunications Conference*, vol. 3, 1996, pp. 1925–1929.

[97] I. S. Amiri and M. Ghasemi, "Design and development of optical dispersion characterization systems." Springer, 2019, p. 9.

[98] S. Ramachandran, "Fiber based dispersion compensation." Springer, 2007, pp. 154–155.

[99] "Intermodal dispersion," https://www.rp-photonics.com/intermodal_dispersion.html, accessed: 2020-11-03.

[100] M. O. R. Hui, "Fiber optic measurement techniques." Academic press, 2009, pp. 394–397.

[101] S. K. Ibrahim and et al, "Novel carrier extraction scheme for phase modulated signals using feed-forward based modulation stripping," *ECOC*, pp. 19–23, 2010.

[102] K. Wu and H. Sun, "Techniques in carrier recovery for optical coherent systems," *OFC/NFOEC Technical Digest of Optical Society of America*, p. OTh4c.3.pdf, 2012.

[103] W. Imajuku and A. Takada, "In-line optical phase-sensitive amplifier with pump light source controlled by optical phase-lock loop," *Journal of Lightwave Technology*, vol. 17, no. 4, pp. 637–646, 1999.

[104] "Method and apparatus for use in carrier recovery in a communications system," https://patents.google.com/patent/US7894333B2/en, accessed: 2020-12-15.

[105] S. Norimatsu, "Optimum optical power splitting ratio of decision driven phase-locked loop in bpsk optical homodyne receiver," *Journal of Lightwave Technology*, vol. 13, no. 11, pp. 2183–2190, 1995.

[106] "Complexity reduced feed forward carrier recovery methods for m-qam modulation formats," https://patents.google.com/patent/US8908809B2/en, accessed: 2020-12-15.

[107] I. Kim and et al, "All-optical carrier synchronization using a phase-sensitive oscillator," *IEEE PHOTONICS TECHNOLOGY LETTERS*, vol. 19, p. 13, 2007.

[108] K. Croussore and G. Li, "Phase and amplitude regeneration of differential phase-shift keyed signals using phase-sensitive amplification," *IEEE Journal of Selected Topics in Quantum Electronics*, vol. 14, no. 3, pp. 648–658, 2008.

[109] M. Qiu and et al, "Simple and efficient frequency offset tracking and carrier phase recovery algorithms in single carrier transmission systems," *Optical Express*, vol. 21, pp. 8157–8165, 2013.

[110] X. Zhou, "Hardware efficient carrier recovery algorithms for single-carrier qam systems," *Advanced Photonics Congress, OSA*, 2012.

[111] S.-L. Lee and et al, "Performance enhancement on soa-based four-wave-mixing wavelength conversion using an assisted beam," *IEEE Photonics Technology Letters*, vol. 14, no. 12, pp. 1713–1715, 2002.

[112] G. Lu and et al, "Format conversion of optical multilevel signals using fwm-based optical phase erasure," *Journal of Lightwave Technology*, vol. 29, no. 16, pp. 2460–2466, 2011.

[113] R. Weerasuriya and et al, "Generation of frequency symmetric signals from a bpsk input for phase sensitive amplification," in *2010 Conference on Optical Fiber Communication (OFC/NFOEC), collocated National Fiber Optic Engineers Conference*, 2010, pp. 1–3.

[114] J. Knab and et al, "Ultrafast carrier dynamics and optical properties of nanoporous silicon at terahertz frequencies," *Optical Materials Express*, vol. 4, no. 2, pp. 300–307, February 2014.

[115] R. Weerasuriya and et al, "Generation of frequency symetric signals from a bpsk input for phase sensitive amplification," *OSA/OFC/NFOEC*, 2010.

[116] J. W. Goodman, "Delta function and fourier transform theorems," in *Introduction to Fourier Optics*. Viva Books Private Limited, 2007, pp. 433–435.

[117] I. J. Nagrath and et al, "Discrete fourier transformation and fast fourier transformation," in *Signals and Systems*. McGraw- Hill, 2003, pp. 260–273.

[118] C. T. Chen, in *Signals and Systems, Third Edition.* Oxford University Press, 2004, pp. 116–190.

[119] L. .Richter and et al, “Linewidth determination from self-heterodyne measurements with subcoherence delay time,” *IEEE Journal of Quantum Electronics*, vol. QE-22, no. 11, pp. 2070–2074, November 1986.

[120] A. Altuncu and A. Cokrak, “Gain and noise figure performance of erbium doped fiber amplifiers(edfa),” *Journal of Electrical and Electronics Engineering*, vol. 04, no. 02, pp. 1111–1122, 2004.

[121] “Erbium-doped fiber amplifiers,” https://www.rp-photonics.com/erbium_doped_fiber_amplifiers.html, accessed: 2020-11-05.

[122] R. Hui, “Optical amplifiers,” in *Introduction to Fiber Optic Communication.* Elsevier, 2019, pp. 179–190.

[123] E. Desurvire, in *Erbium Doped Fiber Amplifiers:Principles and Application.* Wiley Publication, 2002.

[124] A. Ghatak and K. Thyagarajan, “Optical fiber amplifiers,” in *Introduction to Fiber Optics.* Cambridge University Press, 1998, pp. 281–315.

[125] S. Ryu, “Signal linewidth broadening due to nonlinear kerr effect in long-haul coherent system using cascaded optical amplifier,” *Journal of Lightwave technology*, no. 10, pp. 1450 – 1457, 1992.

[126] J. P. Gordon and L. F. Mollenauer, “Phase noise in photonic communications systems using linear amplifiers,” *Optics Letters*, vol. 15, no. 23, pp. 1351–1353, 1990.

[127] G. J. Cowle and et al, “Spectral broadening due to fibre amplifier phase noise,” *Electronics Letters*, vol. 26, no. 7, pp. 424–425, 1990.

[128] E. Desurvire, “Erbium doped fiber amplifiers.” A John Wiley & Sons, Inc., New York, 1993, pp. 399–404.

[129] A. Yariv, in *Optical Electronics (3rd edn).* Reinhart and Winston, New York, 1985.

[130] B. Wang and et al, “Millimeter-resolution long-range ofdr using ultra-linearly 100 ghz-swept optical source realized by injection-locking technique and cascaded fwm process,” *Optics Express*, February 2017.

[131] R.Weerasuriya and et al, "Comparison of frequency symmetric signal generation from a bpsk input using fiber and semiconductor-based nonlinear elements," *IEEE Photonics Technology Letters*, vol. 23, no. 10, pp. 651–653, 2011.